

Functional Adaptive Double-Sparsity Estimator for Functional Linear Regression Model with Multiple Functional Covariates

Cheng Cao

School of Data Science, City University of Hong Kong

Jiguo Cao

Department of Statistics and Actuarial Science, Simon Fraser University

Hailiang Wang

School of Design, The Hong Kong Polytechnic University

Kwok-Leung Tsui

Grado Department of Industrial and Systems Engineering,
Virginia Polytechnic Institute and State University

Xinyue Li

School of Data Science, City University of Hong Kong

July 13, 2023

Abstract

Sensor devices have been increasingly used in engineering and health studies recently, and the captured multi-dimensional activity and vital sign signals can be studied in association with health outcomes to inform public health. The common approach is the scalar-on-function regression model, in which health outcomes are the scalar responses while high-dimensional sensor signals are the functional covariates, but how to effectively interpret results becomes difficult. In this study, we propose a new Functional Adaptive Double-Sparsity (FadDoS) estimator based on functional regularization of sparse group lasso with multiple functional predictors, which can achieve global sparsity via functional variable selection and local sparsity via zero-subinterval identification within coefficient functions. We prove that the FadDoS estimator converges at a bounded rate and satisfies the oracle property under mild conditions. Extensive simulation studies confirm the theoretical properties and exhibit excellent performances compared to existing approaches. Application to a Kinect sensor study that utilized an advanced motion sensing device tracking human multiple joint

movements and conducted among community-dwelling elderly demonstrates how the Fad-DoS estimator can effectively characterize the detailed association between joint movements and physical health assessments. The proposed method is not only effective in Kinect sensor analysis but also applicable to broader fields, where multi-dimensional sensor signals are collected simultaneously, to expand the use of sensor devices in health studies and facilitate sensor data analysis.

Keywords: scalar-on-function regression, Kinect sensor, Sensor device data, sparse group lasso

1 Introduction

Wearable devices have been contributing to wide applications in healthcare, medical, and rehabilitation fields by continuously monitoring and collecting individual’s physical activity and vital signs. With emerging sensing technologies in recent years, a novel sensor device called Kinect has been increasingly used to perform precise three-dimensional movement tracking of 25 skeleton joints, which can unlock the potential of automated health monitoring and enable enhanced healthcare decisions (Gasparrini et al., 2014; Cippitelli et al., 2015; Kohout et al., 2021). In an elderly mobility study conducted in Hong Kong local communities, we collected multi-joint movements using Kinect sensor among the community-dwelling elderly to evaluate their dynamic balance capabilities. Figure 1(a) displays the setup of the Kinect camera and its three-dimensional coordinates for motion capturing. Figure 1(b) depicts the set of all skeletal joints captured. Figure 1(c) provides an example of the captured movement of the sacrum at the base of the spine for 50 participants. The three-dimensional displacement signals $K_x(t)$, $K_y(t)$ and $K_z(t)$ denote the horizontal direction representing swaying motion, the vertical direction representing up-and-down motion, and the walking direction respectively. The sensor records displacement data, from which velocity, and frequency domain data can be calculated to enrich the Kinect sensor dataset. Accurate multi-joint movements provide unprecedented opportunities to analyze the relationship between joint movement patterns and physical health assessments.

However, the analysis of the complex high-dimensional Kinect data, same as other types of multi-dimensional sensor device data, remains challenging. Given a large number of functional covariates and measured scalar responses, we consider scalar-on-function regression model with multiple functional covariates (Ramsay and Silverman, 2005). The estimates of the coefficient functions can yield insights into the detailed associations between functional covariates and the

outcome over the time domain. To enhance the interpretability of the complex model, it is crucial to conduct functional variable selection and further obtain sparse coefficient estimates, which we refer to as global sparsity and local sparsity respectively, to obtain meaningful results and relevant interpretation of the associations (Tu et al., 2012, 2020).

Several estimators targeting scalar-on-function regression model with multiple functional covariates address global sparsity to achieve functional variable selection (Pannu and Billor, 2017; Collazos et al., 2016; Cheng et al., 2020). Gertheiss et al. (2013) proposed a sparsity-smoothness estimator to obtain a parsimonious model based on functional generalization of group lasso penalty (Meier et al., 2009), while Matsui and Konishi (2011) and Mingotti et al. (2013) suggested alternative functional regularizations. However, these estimators without concerning local sparsity can only facilitate the interpretability with respect to variable selection. With increasing attention to coefficient interpretability, more methods aim to preserve local sparsity of functional coefficient (James et al., 2009; Zhou et al., 2013). The sparse estimation of functional coefficient is reformulated to variable selection in basis function representation of linear regression with various regularizations. Wang and Kai (2015) leveraged group bridge (Huang et al., 2009), allowing for overlap between small subregions to induce zero-subregion coefficient estimates, and Lin et al. (2017) proposed an estimator based on the functional generalization of SCAD penalty. In functional linear classification problems, Park et al. (2022) employed functional ℓ_1 -type penalty with

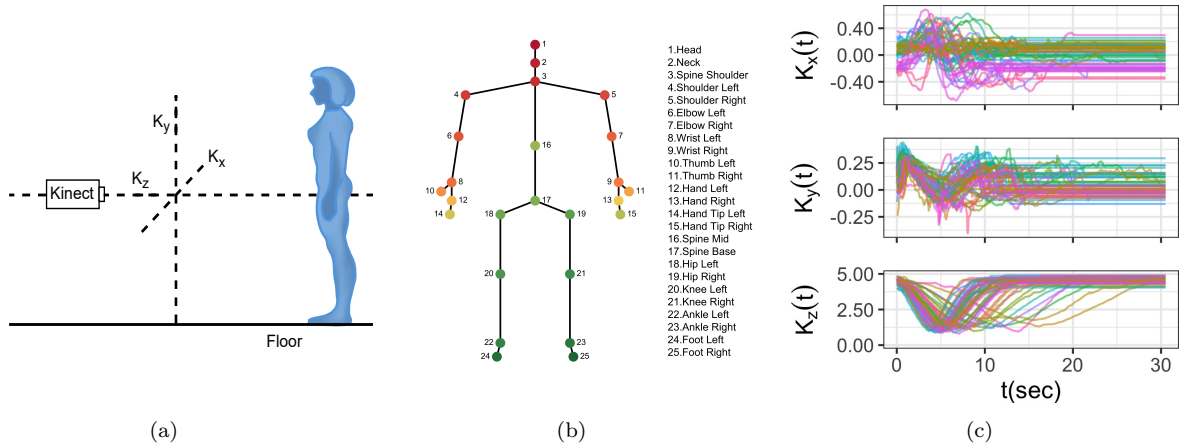


Figure 1: (a) The setup of Kinect sensor. (b) The 25 joints of human skeleton captured by Kinect sensor. (c) The three-dimensional displacement of the sacrum (joint 17: Spine Base) for all participants in Timed Up and Go (TUG) Test. Each curve represents time-dependent sacrum position of a participant during the entire test. Due to the different duration of finishing, we use the last observation to pad the shorter signals till all signals have equal time domain. The participant ID is color coded. Top panel: horizontal direction. Middle panel: vertical direction. Bottom panel: walking direction.

smoothness constraints. These approaches can identify zero subregions and obtain nice asymptotic properties, but both primarily target a single functional covariate. To the best of our knowledge, Tu et al. (2012) and Tu et al. (2020) incorporated the notion of global and local sparsity for multiple functional covariates, while depending on concave group bridge penalty and pitching in other related functional scenarios such as logistics functional regression and time-varying functional regression models for longitudinal data.

In this paper, we propose a novel functional adaptive double-sparsity (FadDoS) estimator, which can achieve global sparsity via functional variable selection and local sparsity via sparse coefficient estimation simultaneously in scalar-on-function regression models with multiple functional covariates. The combination of global and local sparsity is termed double-sparsity. The proposed estimator achieves double-sparsity through functional generalization of sparse group lasso and adaptive penalization. By solving an optimization problem that incorporates regularization and smoothing splines in a single convex objective function, we can provide the estimates of coefficient functions with nice double-sparsity and smoothness control. The benefit of convexity is the guarantee of converging to a local minimum during model fitting.

The major contribution of our work is three-fold. First, we defined an important property, double-sparsity, of functional linear regression with multiple functional covariates, which leads to sparse and consistent functional estimates when not all functional covariates over the entire time domain are associated with the scalar response. Second, we provided a one-stage estimation procedure for the FadDoS estimator to achieve double-sparsity, which is computationally efficient and easy to implement. Third, the accuracy of the estimation is theoretically stable and solid as we prove that the FadDoS estimator converges at an optimal rate and enjoys oracle properties. Our method can remarkably enhance model parsimony and interpretability for high-dimensional sensor device data that existing methods in the literature lack. As an example, the FadDoS estimator can be applied to complex Kinect sensor data to effectively examine the association between joint movements and mobility, based on which automated assessment tools can be further developed for health monitoring and early intervention.

The rest of this paper is organized as follows. In Section 2, we introduce the double-sparsity structure of the scalar-on-function regression model with multiple functional covariates and computation of the FadDoS estimator. Section 3 presents asymptotic properties of the proposed

estimator. Extensive simulation studies are conducted in Section 4 to evaluate the performance of our estimator and compare the results with existing approaches. Section 5 describes the application for the Kinect elderly study. Conclusion and discussion are in Section 6. All code for model implementation and simulation is available in the supplementary material and at <https://github.com/Cheng-0621/FadDoS>.

2 Methodology

2.1 Global and Local Sparsity in Scalar-on-function Regression Model with Multiple Functional Covariates

Suppose that Y_i be the scalar response and $X_{ij}(t) \in L^2(\mathcal{T})$ be the j th functional covariate for subject i observed at time t in domain \mathcal{T} . The functional linear model with multiple functional covariates is thus

$$Y_i = \mu + \sum_{j=1}^J \int_{\mathcal{T}} X_{ij}(t) \beta_j(t) dt + \epsilon_i, \quad i = 1, \dots, n, \quad (1)$$

where μ is the intercept term and $\epsilon_i \sim N(0, \sigma^2)$. The smooth coefficient function $\beta_j(t)$ provides a time-dependent contribution of $X_{ij}(t)$ to the corresponding response Y_i .

We use the following notation: for all measurable functions f whose absolute value raised to the q -th power has a finite integral, which is $\|f\|_q = (\int_{\mathcal{T}} |f(t)|^q dt)^{1/q} < \infty$, and the supremum norm of a function f is defined as $\|f\|_{\infty} = \sup_{t \in \mathcal{T}} |f(t)|$. The double-sparsity structure of the functional linear model (1) contains both global sparsity and local sparsity. Mathematically, the global sparsity is characterized by the set of indices for which functional covariates have no contribution to the response over the entire domain, i.e. $\{j \in \{1, \dots, J\} : \beta_j(t) = 0, \text{ for all } t \in \mathcal{T}\}$, while for those functional covariates not belonging to this set, the local sparsity is depicted by the partition of zero and nonzero subregion of the corresponding coefficient functions. Suppose a subregion $I \subset \mathcal{T}$, the zero subregion is defined $N_0(\beta_j) = \{I \subset \mathcal{T} : \beta_j(t) = 0, \text{ for all } t \in I\}$ and thus the nonzero subregion $N_1(\beta_j)$ is the complement of $N_0(\beta_j)$. It implies that within the subinterval $N_0(\beta_j)$, the functional covariate has no effect on the response. With the double-sparsity structure, important functional predictors can be selected and nonzero subintervals can be further identified.

2.2 Functional Sparse Group Lasso Penalization

To achieve both global and local sparsity, we propose a novel regularization method based on functional generalization of sparse group lasso (fSGL), where SGL is initially proposed by Friedman et al. (2010) and Simon et al. (2013). The penalty function is

$$P_{\lambda_1, \lambda_2, \varphi}(\boldsymbol{\beta}) = \lambda_1 \|\boldsymbol{\beta}\|_1 + \lambda_2 \sum_{j=1}^J (\|\beta_j\|_2^2 + \varphi \|\mathcal{D}^m \beta_j\|_2^2)^{1/2}, \quad (2)$$

where $\boldsymbol{\beta} = (\beta_1, \dots, \beta_J)^T$ is the vector of coefficient functions, $\|\boldsymbol{\beta}\|_1 = \sum_{j=1}^J \|\beta_j\|_1$ with $\|\beta_j\|_1 = \int_{\mathcal{T}} |\beta_j(t)| dt$, $\|\beta_j\|_2^2 = \int_{\mathcal{T}} |\beta_j(t)|^2 dt$ and $\|\mathcal{D}^m \beta_j\|_2^2 = \int_{\mathcal{T}} |\partial^m \beta_j(t) / \partial t^m|^2 dt$ such that $m \leq d$, where d is the degree of polynomial functions, $\lambda_1, \lambda_2, \varphi \geq 0$. The additive penalties contain two convex regularizations. The functional generalization of ℓ_1 (functional ℓ_1) penalty regularizes the magnitude of local sparseness, while functional generalization of $\ell_{1,2}$ (functional $\ell_{1,2}$) penalty manages global sparseness. Within functional $\ell_{1,2}$ penalty, the roughness penalty $\varphi \|\mathcal{D}^m \beta_j\|_2^2$ is employed to apply penalization to the m -th order derivative of the j th coefficient function to control the smoothness of estimated nonzero coefficient functions. The minimizer of mean squared loss function regularized by fSGL in Equation (2) is called functional double-sparsity (FDoS) estimator.

However, one drawback of this regularization method is that the magnitude of penalization is the same for all functional covariates in the model, which may result in either insufficient suppression of zero functional estimates or underestimation of nonzero functional estimates. Theoretically, the equal degrees of penalization fail to satisfy the oracle property suggested in Fan and Li (2001), unless a proper adaptive method is applied to enable importance re-weighting of different coefficient functions (Zou, 2006).

2.3 Functional Adaptive Double-Sparsity Estimator

We further enhance the fSGL penalization with adaptive weights to allow for flexible regularization to different coefficient functions. The adaptive penalty function is

$$P_{\lambda_1, \lambda_2, \varphi}(\boldsymbol{\beta}) = \lambda_1 \sum_{j=1}^J w_j^{(1)} \|\beta_j\|_1 + \lambda_2 \sum_{j=1}^J w_j^{(2)} (\|\beta_j\|_2^2 + \varphi \|\mathcal{D}^m \beta_j\|_2^2)^{1/2}, \quad (3)$$

where $w_j^{(1)} = \|\check{\beta}_j\|_1^{-a}$ and $w_j^{(2)} = \|\check{\beta}_j\|_2^{-a}$ are known nonnegative weights and $\check{\beta}_j$ is the initial estimator, $a > 0$ is an adjustment of the adaptive weights and usually $a = 1$.

Intuitively, the adaptive weights can incorporate prior insights into functional covariates: a larger value implies less importance in the model. The adaptive approach can effectively penalize zero functions to reduce false negatives without over-regularizing nonzero functions. Additionally, the adaptive weights in Equation (3) are predictor-wise rather than subregion-wise, i.e., $\|w_j^{(1)}\beta_j\|_1$ with known nonnegative weight function $w_j^{(1)}(t) = |\check{\beta}_j(t)|^{-a}$. We do not choose subregion-wise weight because it is computationally intensive and more importantly, prone to errors, as the coefficient estimation is largely affected by choices of initial estimators. While the adaptive estimation allows for different initial estimators, we choose the smoothing spline estimator as in Cardot et al. (2003) with the second-order differential operator in the penalty derived from functional generalization of ridge penalization with generally no sparse solution, to avoid explosion to infinity when calculating the reciprocal of the norm even for those less significant functional covariates.

Given the adaptive fSGL penalization in Equation (3), we propose the FadDoS estimator, which minimizes the penalized mean squared loss defined by

$$L_n(\beta, \mu) = \frac{1}{2} \sum_{i=1}^n \left[Y_i - \mu - \sum_{j=1}^J \int_{\mathcal{T}} X_{ij}(t) \beta_j(t) dt \right]^2 + \lambda_1 \sum_{j=1}^J w_j^{(1)} \|\beta_j\|_1 + \lambda_2 \sum_{j=1}^J w_j^{(2)} (\|\beta_j\|_2^2 + \varphi \|\mathcal{D}^m \beta_j\|_2^2)^{1/2}. \quad (4)$$

It is obvious that FDoS is a special case of FadDoS if fixing $w_j^{(1)} = w_j^{(2)} = 1$ for all $j = 1, \dots, J$. Moreover, $m = 2$ is commonly chosen and we adopt it for the rest of the paper.

The computational procedure of the FadDoS estimator is shown below. We first express the coefficient functions $\beta_j(t)$ with B-splines. Suppose that there are $M_n + 1$ equally spaced knots $0 = t_{j0} < t_{j1} < \dots < t_{jM_n} = T$ in the domain \mathcal{T} and d degree of polynomial functions, and let \mathcal{S}_j be the linear space spanned by basis functions $\{B_{jk}(t) : k = 1, \dots, M_n + d\}$ in \mathcal{T} , we have $\beta_j(t) = \sum_{k=1}^{M_n+d} B_{jk}(t) b_{jk} = \mathbf{B}_j^T(t) \mathbf{b}_j$, where $\mathbf{B}_j(t) = (B_{j1}(t), \dots, B_{j(M_n+d)}(t))^T$, $\mathbf{b}_j = (b_{j1}, \dots, b_{j(M_n+d)})^T$. With the compact support property of B-splines, the basis function can characterize the sparseness of coefficient functions as it is a nonzero polynomial over no more than $d + 1$ adjacent subintervals $[t_{j(r-d-1)}, t_{jr})$, $r \in \{1, \dots, M_n\}$, implying only $d + 1$ basis functions

have supports within a subinterval $[t_{j(r-1)}, t_{jr})$.

Using B-spline basis functions, we reparameterize Equation (4) to facilitate computation. First, $\|\beta_j(t)\|_1$ can be represented by basis coefficients according to B-spline properties (De Boor, 2001; Mingotti et al., 2013). Mathematically, let $\Delta_n = t_{jr} - t_{j(r-1)}$, $\|\beta_j(t)\|_1 \approx \Delta_n \sum_{k=1}^{M_n+d} |b_{jk}| = \Delta_n \|\mathbf{b}_j\|_1$. Hence, functional ℓ_1 penalty term can be replaced by $\Delta_n \sum_{j=1}^J \|\mathbf{b}_j\|_1$. Additionally, the functional $\ell_{1,2}$ penalty term can be rewritten as $\sum_{j=1}^J (\|\beta_j\|_2^2 + \varphi \|\mathcal{D}^2 \beta_j\|_2^2)^{1/2} = \sum_{j=1}^J (\mathbf{b}_j^T (\boldsymbol{\Phi}_j + \varphi \boldsymbol{\Omega}_j) \mathbf{b}_j)^{1/2}$, where $\boldsymbol{\Phi}_j$ is a $(M_n + d) \times (M_n + d)$ matrix with the (p, q) element equal to $(\boldsymbol{\Phi}_j)_{pq} = \int B_{jp}(t) B_{jq}(t) dt$, and $\boldsymbol{\Omega}_j$ is also a $(M_n + d) \times (M_n + d)$ matrix with the (p, q) element equal to $(\boldsymbol{\Omega}_j)_{pq} = \int B_{jp}^{(2)}(t) B_{jq}^{(2)}(t) dt$. In practice, with dense grids observed over the domain \mathcal{T} , we compute $(\boldsymbol{\Phi}_j)_{pq} \approx \Delta_n \sum_r B_{jp}(t_{jr}) B_{jq}(t_{jr})$ and $(\boldsymbol{\Omega}_j)_{pq} \approx \Delta_n \sum_r B_{jp}^{(2)}(t_{jr}) B_{jq}^{(2)}(t_{jr})$. Let $\mathbf{K}_j = (\boldsymbol{\Phi}_j + \varphi \boldsymbol{\Omega}_j) / \Delta_n^2$, and we can use Cholesky decomposition to have $\mathbf{K}_j = \mathbf{L}_j \mathbf{L}_j^T$, where \mathbf{L}_j is a $(M_n + d) \times (M_n + d)$ non-singular lower triangular matrix. By defining a new vector of coefficients $\tilde{\mathbf{b}}_j = \Delta_n \mathbf{L}_j^T \mathbf{b}_j$ and $\tilde{\mathbf{b}} = (\tilde{\mathbf{b}}_1^T, \dots, \tilde{\mathbf{b}}_J^T)^T$, we obtain the equivalent matrix form of the objective function in Equation (4),

$$L_n(\tilde{\mathbf{b}}, \boldsymbol{\mu}) = \frac{1}{2} \|\mathbf{Y} - \boldsymbol{\mu} - \sum_{j=1}^J \tilde{\mathbf{U}}_j \tilde{\mathbf{b}}_j\|_2^2 + \lambda_1 \sum_{j=1}^J w_j^{(1)} \|(\mathbf{L}_j^T)^{-1} \tilde{\mathbf{b}}_j\|_1 + \lambda_2 \sum_{j=1}^J w_j^{(2)} \|\tilde{\mathbf{b}}_j\|_2, \quad (5)$$

where $\mathbf{Y} = (Y_1, \dots, Y_n)^T$, $\boldsymbol{\mu} = \mu \mathbf{1}_n$, $\mathbf{1}_n = (1, \dots, 1)^T$ denotes a n -vector of ones. $\tilde{\mathbf{U}}_j = \mathbf{U}_j (\mathbf{L}_j^T)^{-1} / \Delta_n$ where \mathbf{U}_j is an $n \times (M_n + d)$ matrix with entries $(\mathbf{U}_j)_{ip} = \int_{\mathcal{T}} X_{ij}(t) B_{jp}(t) dt$ that can be approximated by $\Delta_n \sum_r X_{ij}(t_{jr}) B_{jp}(t_{jr})$. The solution to the FadDoS estimator of $\hat{\beta}_j(t)$ is thus $\hat{\beta}_j(t) = \Delta_n^{-1} \mathbf{B}_j^T (\mathbf{L}_j^T)^{-1} \tilde{\mathbf{b}}_j^*$ and the objective turns to estimate $\tilde{\mathbf{b}}_j^*$.

2.4 Algorithm

The algorithm for solving Equation (5) was developed based on Alternating Direction Method of Multipliers (ADMM). ADMM is effective in lasso and group lasso, and has been recently extended to non-separable and non-smooth convex problems such as fused lasso, as it is powerful in leveraging the complicated structure of ℓ_1 norm (Boyd et al., 2010; Li et al., 2014; Beer et al., 2019). Here we choose ADMM because it does not require a differentiable objective function and at the same time supports decomposition to split the objective into solvable subproblems.

We first define two common operators: for $\lambda, \kappa > 0$ and $y \in \mathbb{R}^p$, the soft thresholding operator $S_{1, \lambda/\kappa}(y) = \text{sgn}(y)(|y| - \lambda/\kappa)_+$ and $S_{2, \lambda/\kappa}(y) = y / \|y\|_2 (\|y\|_2 - \lambda/\kappa)_+$. For ease of notation, we

assume no intercept, i.e., $\mu = 0$ and consider $w_j^{(1)} = w_j^{(2)} = 1$ for all j to illustrate the main idea, which is equivalent to the FDoS estimator. The estimate of μ for the case $\mu \neq 0$ is shown at the end of the section. Let \mathbf{D} be a block diagonal matrix, $\mathbf{D} = \text{diag}((\mathbf{L}_1^T)^{-1}, (\mathbf{L}_2^T)^{-1}, \dots, (\mathbf{L}_J^T)^{-1})$, the optimization problem in Equation (5) can be rewritten as

$$\begin{aligned} \min_{\tilde{\mathbf{b}}_j \in \mathbb{R}^{M_n+d}, j=1, \dots, J} \quad & \frac{1}{2} \|\mathbf{Y} - \sum_{j=1}^J \tilde{\mathbf{U}}_j \tilde{\mathbf{b}}_j\|_2^2 + \lambda_1 \|\mathbf{z}\|_1 + \lambda_2 \sum_{j=1}^J \|\tilde{\mathbf{b}}_j\|_2 \\ \text{s.t.} \quad & \mathbf{z} = \mathbf{D} \tilde{\mathbf{b}} \end{aligned} \quad (6)$$

and the corresponding augmented Lagrangian function $\mathcal{L}(\tilde{\mathbf{b}}, \mathbf{z}, \mathbf{u}) = \frac{1}{2} \|\mathbf{Y} - \sum_{j=1}^J \tilde{\mathbf{U}}_j \tilde{\mathbf{b}}_j\|_2^2 + \lambda_1 \|\mathbf{z}\|_1 + \lambda_2 \sum_{j=1}^J \|\tilde{\mathbf{b}}_j\|_2 + \mathbf{u}^T (\mathbf{D} \tilde{\mathbf{b}} - \mathbf{z}) + \rho/2 \|\mathbf{D} \tilde{\mathbf{b}} - \mathbf{z}\|_2^2$, where $\rho > 0$ is the prespecified augmented Lagrangian parameter, namely the step size to update the dual variable. The iteration scheme of ADMM consists of three sub-problems shown below.

First, we deal with the $\tilde{\mathbf{b}}$ -update at the k th iteration. Since the penalty terms are separable, we can update $\tilde{\mathbf{b}}_j^{k+1}$ parallelly at the k th iteration. Assuming other coefficients fixed, we define $\mathbf{r}_{(-l)} = \mathbf{Y} - \sum_{j \neq l} \tilde{\mathbf{U}}_j \tilde{\mathbf{b}}_j^k$, $\mathbf{z}^k = ((\mathbf{z}_1^k)^T, \dots, (\mathbf{z}_J^k)^T)^T$ and $\mathbf{u}^k = ((\mathbf{u}_1^k)^T, \dots, (\mathbf{u}_J^k)^T)^T$, then

$$\begin{aligned} \tilde{\mathbf{b}}_l^{k+1} = \arg \min_{\tilde{\mathbf{b}}_l \in \mathbb{R}^{M_n+d}} \quad & \frac{1}{2} \|\mathbf{r}_{(-l)} - \tilde{\mathbf{U}}_l \tilde{\mathbf{b}}_l\|_2^2 + \lambda_2 \|\tilde{\mathbf{b}}_l\|_2 + (\mathbf{u}_l^k)^T ((\mathbf{L}_l^T)^{-1} \tilde{\mathbf{b}}_l - \mathbf{z}_l^k) + \\ & \rho/2 \|(\mathbf{L}_l^T)^{-1} \tilde{\mathbf{b}}_l - \mathbf{z}_l^k\|_2^2. \end{aligned} \quad (7)$$

To further solve the optimization problem, we employ a linearization technique to approximate the quadratic term efficiently (Wang and Yuan, 2012), and details of derivation are provided in the supplementary file. We let $\hat{\mathbf{U}}_l = (\tilde{\mathbf{U}}_l^T, \rho^{1/2} \mathbf{L}_l^{-1})^T$ and $\hat{\mathbf{r}}_{(-l)}^k = (\mathbf{r}_{(-l)}^T, \rho^{1/2} (\mathbf{z}_l^k + \mathbf{u}_l^k/\rho)^T)^T$, and thus the $\tilde{\mathbf{b}}$ -update solution is computed by the second operator such that $\tilde{\mathbf{b}}_l^{k+1} = S_{2, \lambda_2/\nu_l}(\tilde{\mathbf{b}}_l^k - \hat{\mathbf{U}}_l^T (\hat{\mathbf{U}}_l \tilde{\mathbf{b}}_l^k - \hat{\mathbf{r}}_{(-l)}^k)/\nu_l)$, where $\nu_l > 0$ is the proximal parameter that controls the proximity to $\tilde{\mathbf{b}}_l^k$. Note that ν_l is required to be larger than the spectral radius of $\tilde{\mathbf{U}}_l^T \tilde{\mathbf{U}}_l + \rho \mathbf{I}$ for convergence (Wang and Yuan, 2012).

Second, the \mathbf{z} -update at the k th iterations is

$$\mathbf{z}^{k+1} = \arg \min_{\mathbf{z} \in \mathbb{R}^{J \times (M_n+d)}} \lambda_1 \|\mathbf{z}\|_1 + (\mathbf{u}^k)^T (\mathbf{D} \tilde{\mathbf{b}}^{k+1} - \mathbf{z}) + \rho/2 \|\mathbf{D} \tilde{\mathbf{b}}^{k+1} - \mathbf{z}\|_2^2. \quad (8)$$

Algorithm 1 ADMM FDoS

Parameters $\lambda_1, \lambda_2, \varphi$

Initialize $\tilde{\mathbf{b}}^0, \mathbf{z}^0, \mathbf{u}^0$

for $k = 1, 2, \dots$, **do**

for $l = 1, 2, \dots, J$ **do**

 Let ν_l be the spectral radius of $\tilde{\mathbf{U}}_l^T \tilde{\mathbf{U}}_l + \rho \mathbf{I}$ multiplied by 5

 Compute $\tilde{\mathbf{b}}_l^{k+1} = S_{2, \lambda_2 / \nu_l}(\tilde{\mathbf{b}}_l^k - \tilde{\mathbf{U}}_l^T (\tilde{\mathbf{U}}_l \tilde{\mathbf{b}}_l^k - \hat{\mathbf{r}}_{(-l)}^k)) / \nu_l$

end for

 Compute $\mathbf{z}^{k+1} = S_{1, \lambda_1 / \rho}(\mathbf{D} \tilde{\mathbf{b}}^{k+1} + \mathbf{u}^k / \rho)$

 Compute $\mathbf{u}^{k+1} = \mathbf{u}^k + \rho(\mathbf{D} \tilde{\mathbf{b}}^{k+1} - \mathbf{z}^{k+1})$

end for until stopping criteria with a pre-specified tolerance ϵ_{tol} such that

$$\|\tilde{\mathbf{b}}^k - \tilde{\mathbf{b}}^{k-1}\|_2 / \max\{\|\tilde{\mathbf{b}}^k\|_2, 1\} \leq \epsilon_{\text{tol}}$$

is reached

Output \mathbf{z}^* and $\tilde{\mathbf{b}}^* = \mathbf{D}^{-1} \mathbf{z}^*$

The \mathbf{z} -update solution is computed by the first operator such that $\mathbf{z}^{k+1} = S_{1, \lambda_1 / \rho}(\mathbf{D} \tilde{\mathbf{b}}^{k+1} + \mathbf{u}^k / \rho)$.

Details of derivation are given in the supplementary file.

Third, the dual variable update at the k th iteration is $\mathbf{u}^{k+1} = \mathbf{u}^k + \rho(\mathbf{D} \tilde{\mathbf{b}}^{k+1} - \mathbf{z}^{k+1})$.

The full algorithm is described in Algorithm 1. When $\mu \neq 0$, we can estimate $\hat{\mu}^{k+1}$ after \mathbf{z} -update at the k th iteration by computing $\hat{\mu}^{k+1} = n^{-1} \mathbf{1}_n^T (\mathbf{Y} - \tilde{\mathbf{U}} \mathbf{D}^{-1} \mathbf{z}^{k+1})$ until the stopping criteria is reached. In addition, the set of three tuning parameters is determined by cross-validation, assuming ρ prespecified, M_n and d fixed.

3 Asymptotic Properties

Under some regularity conditions, we show that the proposed estimator converges to the true coefficient function in a bounded rate. As with other lasso-like problems, the FDoS estimator fails to satisfy the oracle property unless with appropriate adaptive penalization. Therefore, it can be shown that the FadDoS estimator fulfills the property under mild conditions of an initial estimator. To demonstrate the asymptotic behaviors, the following assumptions are required:

(A.1) $\|\mathbf{X}\|_2 \leq c_1 < \infty$ almost surely for some constant c_1 .

(A.2) $\beta(t)$ satisfies Hölder condition: $|\beta^\xi(t_1) - \beta^\xi(t_2)| \leq c_2 |t_1 - t_2|^\zeta$ for some constant c_2 , and $t_1, t_2 \in \mathcal{T}$. We denote $\delta \stackrel{\text{def}}{=} \xi + \zeta$ and assume that $2 \leq \delta \leq d$, where d is the degree of B-splines.

Assumptions (A.1) and (A.2) are identical with (H1) and (H3) of Cardot et al. (2003). (A.2) requires the coefficient function $\beta(t)$ to be sufficiently smooth.

Recall that λ_1 , λ_2 , and φ are tuning parameters for the proposed estimators. For simplicity of the conditions, we choose $\varphi = \lambda_2^2$ to reduce the number of tuning parameters. We assume λ_1 and λ_2 are varying with n under the following conditions.

(A.3) The growth of M_n is located within a loose upper-bound $M_n = o(n^{1/5})$ and lower-bound $M_n = \omega(n^{1/(2\delta+1)})$ which is defined as $M_n/n^{1/(2\delta+1)} \rightarrow \infty$ as n tends to infinity. Additionally, the conditions for choosing values of tuning parameters are $\lambda_1 = o(1)$ and $\lambda_2 = o(1)$.

The first theoretical result demonstrates that our proposed estimator converges at an optimal rate in approximating the true function. It is proved through the estimation error between the proposed estimator and B-spline approximant $\beta_{l\alpha}(t)$ from the family of \mathcal{S} for $l = 1, \dots, J$, which can converge to the true function from De Boor (2001) (see more details in Lemma 1 of supplementary materials). It is further noted that the B-spline approximant can preserve the sparsity of the true function because basis coefficients can be equal to zero if the support of the corresponding basis function falls in the zero subregion $N_0(\beta_j)$. Thus, the asymptotic behavior of the proposed estimator is stated in the following theorem.

Theorem 1 (Convergence) *Under (A.1)-(A.3), if $\lambda_1\phi_1 = O(n^{-1/2})$ and $\lambda_2\phi_2 = O(n^{-1/4})$, $\|\hat{\beta}_l - \beta_l\|_\infty = O_p(M_n^{1/2}n^{-1/2})$, $l = 1, \dots, J$, where $\phi_1 = \phi_2 = 1$ for FDoS, $\phi_1 = \sup_{l \in \mathcal{A}} \|\check{\beta}_l\|_1^{-a}$ and $\phi_2 = \sup_{l \in \mathcal{A}} \|\check{\beta}_l\|_2^{-a}$ are stochastic quantities for FadDoS.*

The above theorem highlights that there always exists a local solution $\hat{\beta}_l(t)$ for the l th functional covariate with probability approaching one, while the convergence rate is bounded by $O_p(M_n^{1/2}n^{-1/2})$.

The oracle property of the functional linear model with multiple functional covariates can be stated under the double-sparsity structure. For global sparsity, the estimator can identify all true nonzero coefficient functions with probability approaching one. For local sparsity, the estimator further recovers zero subregions with probability approaching one and is asymptotically pointwise normally distributed. The oracle property is satisfied in a double-asymptotic framework, indicating that the number of basis functions diverges with the sample size, i.e. $M_n \rightarrow \infty$ as $n \rightarrow \infty$, but M_n grows at a slower rate than n . With the support of B-splines, one can always efficiently

reduce infinite-dimensional models to low-dimensional scenarios, where the number of parameters is smaller than the sample size.

For illustrating the oracle property we divide coefficient function $\beta_l(t)$ into two regions: $I_1(\beta_l) = \{I \subset \mathcal{T} : \sup |\beta_l(t)| > D_l M_n^{-\delta}, \text{ for all } t \in I\}$ for some positive constant D_l , and the complementary part is $I_0(\beta_l) = \{I \subset \mathcal{T} : 0 \leq \sup |\beta_l(t)| \leq D_l M_n^{-\delta}, \text{ for all } t \in I\}$. It is clearly that the zero subregion $N_0(\beta_l)$ is the subset of $I_0(\beta_l)$ for sufficient large D_l . We further define \mathcal{B} as the set consisting of k basis coefficients whose corresponding basis functions $B_k(t)$ have support inside $I_1(\beta_l)$, i.e., $\{k \in \{1, \dots, M_n + d\} : b_k \neq 0\}$. Let $\mathcal{A} = \{l = \{1, \dots, J\} : \sup |\beta(t)| > D_l M_n^{-\delta}, \text{ for all } t \in \mathcal{T}\}$ be the group of nonzero coefficient functions.

Define $\mathbf{C}_l = (M_n/n)\mathbf{U}_l^T \mathbf{U}_l$ and $\mathbf{W}_l \sim N(\mathbf{0}, \sigma^2 \mathbf{C}_l)$, where \mathbf{C}_l is a $(M_n + d) \times (M_n + d)$ positive-definite matrix. Let $\boldsymbol{\alpha}_t$ be a vector of basis coefficient corresponding to B-spline approximant $\beta_{l\alpha}(t)$ mentioned above, the following theorems are developed for the FDoS estimator.

Theorem 2 Under (A.1)-(A.3), if $\lambda_1(nM_n)^{-1/2} \rightarrow \gamma_1$, $\lambda_2^2 n^{-1/2} \rightarrow \gamma_2$,

$$(n/M_n)^{1/2}(\hat{\beta}_l(t) - \beta_l(t)) \xrightarrow{d} \mathbf{B}_l^T(t) \arg \min_{\mathbf{v} \in \mathbb{R}^{M_n+d}} V_1^{(l)}(\mathbf{v}), \quad l = 1, \dots, J,$$

where $V_1^{(l)}(\mathbf{v}) = \mathbf{v}^T \mathbf{C}_l \mathbf{v} - 2\mathbf{W}_l^T \mathbf{v} + \gamma_1 \Gamma(\mathbf{v}) + \gamma_2 \Gamma_2(\mathbf{v})$, $\Gamma_1(\mathbf{v}) = \sum_{k=1}^{M_n+d} \{|v_k| \mathbb{I}(\alpha_{lk} = 0) + v_k \text{sgn}(\alpha_{lk}) \mathbb{I}(\alpha_k \neq 0)\}$ and $\Gamma_2(\mathbf{v}) = \|\mathbf{v}\|_2 \mathbb{I}(\boldsymbol{\alpha}_l = \mathbf{0}) + (\mathbf{v}^T \boldsymbol{\alpha}_l / \|\boldsymbol{\alpha}_l\|_2) \mathbb{I}(\boldsymbol{\alpha}_l \neq \mathbf{0})$.

As stated in Theorem 2, the FDoS estimator does not follow pointwise normal distribution. However, one can find that the limiting distribution of the vector basis coefficient is the same as non-adaptive version of the SGL estimator in Poignard (2018).

Theorem 3 (Double-Sparsity of FDoS) Under (A.1)-(A.3), if $\lambda_1(nM_n)^{-1/2} \rightarrow \gamma_1$, $\lambda_2^2 n^{-1/2} \rightarrow \gamma_2$, FDoS estimator satisfies the following:

1. $\lim_{n \rightarrow \infty} P(\hat{\mathcal{A}}_n = \mathcal{A}) < 1$;
2. For $t \in I_0(\beta_l)$ such that $l \in \mathcal{A}$, $P(\hat{\beta}_l(t) = 0) < 1$.

Theorem 3 demonstrates that neither global nor local selection is consistent as the sparsity structures cannot be recovered with high probability. An appropriate adaptive penalization discussed in Section 2.3 is a promising way to address this issue. Since only predictor-wise adaptive

weights are used, the FadDoS estimator is theoretically different from adaptive SGL in the standard linear model in Poignard (2018). The below theorem shows that FadDoS still enjoys the oracle property if we can ensure that adaptive weights do not approach infinity at a fast rate. The initial estimator is chosen to be the smoothing spline estimator proposed by Cardot et al. (2003), the convergence of which is also ensured. Therefore, the condition is not too stringent because the initial estimator is in fact the ridge estimator in the functional case and therefore the reciprocal of its norm will generally be finite as described before.

Theorem 4 (Oracle Property of FadDoS) *Under (A.1)-(A.3) and mild conditions of the initial estimator, if $\lambda_1(nM_n)^{-1/2} \rightarrow 0$ and $\lambda_2^2 n^{-1/2} \rightarrow 0$; $\lambda_1 n^{(a-1)/2}/M_n^{(a+1)/2} \rightarrow \infty$ and $\lambda_2^2 n^{(a-1)/2}/M_n^{a/2} \rightarrow \infty$, the FadDoS estimator satisfies the following:*

1. (Consistency of global variable selection) $\lim_{n \rightarrow \infty} P(\hat{\mathcal{A}}_n = \mathcal{A}) = 1$.

(Consistency of local zero-subregion identification) For $t \in I_0(\beta_l)$ and $l \in \mathcal{A}$, $\lim_{n \rightarrow \infty} P(\hat{\beta}_l(t) = 0) = 1$.

2. For $t \in I_1(\beta_l)$, we have $(n/M_n)^{1/2}(\hat{\beta}_l(t) - \beta_l(t)) \xrightarrow{d} N(0, \Sigma_{lt})$, where $\Sigma_{lt} = \sigma^2 \mathbf{B}_l^T(t) \mathbf{C}_{l\mathcal{B}\mathcal{B}}^{-1} \mathbf{B}_l(t)$ is the covariance matrix knowing the true subset model, where $\mathbf{C}_{l\mathcal{B}\mathcal{B}}$ be the sub-matrix only with column indices in \mathcal{B} .

4 Simulation

We conduct extensive simulation studies to illustrate the global sparsity and local sparsity of the proposed method and compare it with existing methods to evaluate the model performance.

The true functional linear model is $Y_i = \sum_{j=1}^{10} \int_0^1 X_{ij}(t) \beta_j(t) dt + \epsilon_i$, $i = 1, \dots, n$, where $\epsilon_i \sim N(0, 1)$. We generate functional covariates $X_{ij}(t)$ by letting $X_{ij}(t) = \sum_k a_{ijk} B_{jk}(t)$, $t \in [0, 1]$, where $a_{ij} \sim N(0, 1)$ and $B_{jk}(t)$ is a B-spline basis function defined by order 4 and 50 equally spaced knots. Three different types of coefficient functions are considered, each representing a unique condition:

- (i) $\beta_1(t)$ has a zero subregion $\beta_1(t) = 2 \sin(3\pi t)$ for $0 \leq t \leq 1/3$; $\beta_1(t) = 0$ for $1/3 < t < 2/3$; $\beta_1(t) = -2 \sin(3\pi t)$, for $2/3 \leq t \leq 1$;
- (ii) $\beta_2(t)$ has no zero subregion but two crossings at zero, such that $\beta_2(t) = 1.5t^2 + 2 \sin(3\pi t)$;
- (iii) $\beta_j(t) = 0$ for $j = 3, \dots, 10$, indicating that the functional covariate has no contribution to the

response throughout the entire time domain. We independently simulate 100 replicates with the sample size $n = 100, 200, 300$.

The performance of the estimator is evaluated from two aspects reflecting the realization of global sparsity and local sparsity respectively. The global sparsity, which is equivalent to functional variable selection, can be assessed by true negative rate (TNR) representing the proportion of insignificant functional covariates accurately excluded from the model. For local sparsity, we use integrated squared error (ISE) to measure the difference between the estimate and the underlying truth, defined as $\text{ISE}(\hat{\beta}_j) = (1/|\mathcal{T}|) \int_{\mathcal{T}} (\hat{\beta}_j(t) - \beta_j(t))^2 dt$. It can be further decomposed into $\text{ISE}_0(\hat{\beta}_j)$ and $\text{ISE}_1(\hat{\beta}_j)$ for local zero subregion $N_0(\beta_j)$ and nonzero subregion $N_1(\beta_j)$. The local sparsity can be evaluated via ISE_0 . Additionally, predictive performance measured by prediction mean squared error (PMSE) on the testing data set is also critical to examine the effectiveness of the estimator.

4.1 Tuning Parameter Effects

Figure 2 shows how the FadDoS estimator of $\beta_1(t)$ is affected by tuning parameters. Similar results are observed for $\beta_2(t)$ and displayed in Figure S2. An increase in the local sparsity parameter λ_1 can lead to stronger penalization on adjacent nonzero estimates and yield wider locally sparse subintervals, which can provide flexibility in the control of local sparseness. Moreover, the global sparsity parameter λ_2 primarily administers the overall sparseness of the functional estimates, thereby achieving functional variable selection. As the roughness penalty is embedded in the functional $\ell_{1,2}$ penalty, λ_2 is also involved in smoothness control, same as the smoothing parameter φ , which measures the total curvature and ensures smoothness.

Table 1 further provides quantitative evaluation of tuning parameter effects. It is not surprising that FadDoS shrinks $\hat{\beta}_1(t)$ in zero subregion and all $\hat{\beta}_j(t)$, $j = 3, \dots, 10$ towards zero by increasing λ_1 and λ_2 , while the procedure delivers exactly the opposite results regarding nonzero subregions of $\hat{\beta}_1(t)$ and $\hat{\beta}_2(t)$. The combination of λ_1 and λ_2 provides an elastic-net-like estimation balancing zero and nonzero regions of coefficient functions. Thus the minimization of PMSE and ISE are produced under the trade-off between local and global sparsity parameters.

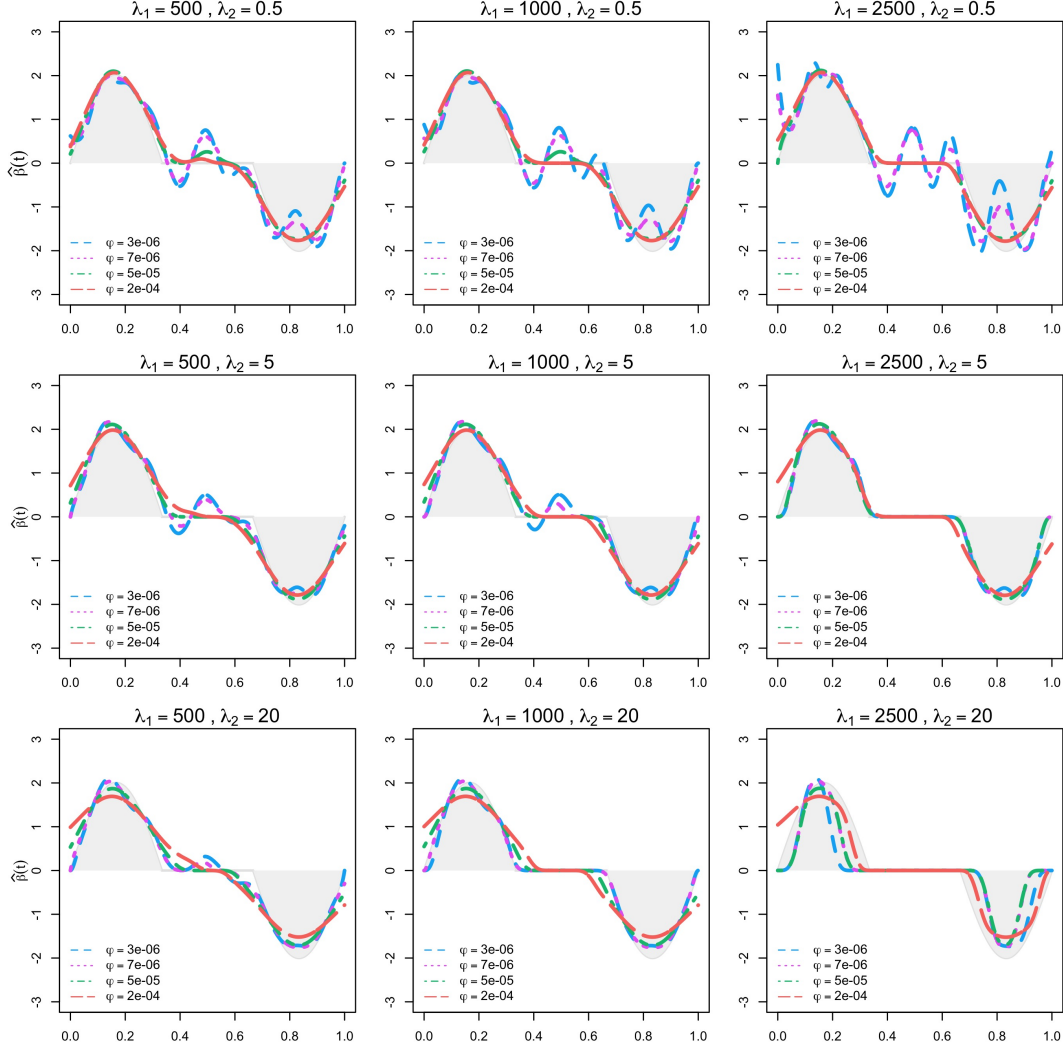


Figure 2: Estimated coefficient functions for $\beta_1(t)$ using FadDoS with varying tuning parameters. The sample size is $n = 200$.

4.2 Comparison to Existing Methods

We compare our proposed estimators with the aforementioned estimation methods f-GL (Gertheiss et al., 2013), fLARS (Cheng et al., 2020), and SLoS (Lin et al., 2017), and tuning parameters for all estimators are selected by 5-fold cross-validation to ensure optimal performance of each estimator.

As shown in Figure 3, the FadDoS estimator fits the shape of the peak and the valley well. Table 2 summarizes PMSE and ISE of all estimators. It is expected that our proposed estimators and SLoS have better performance in zero subregions than f-GL and fLARS which only take functional covariate selection into account. The locally sparse estimates by FDoS and FadDoS are attributed to the nice shrinkage property of the functional ℓ_1 penalty term. This can also be

φ	$\lambda_1 \backslash \lambda_2$	PMSE ($\times 10^{-2}$)			ISE ₀ ($\hat{\beta}_1$)			ISE ₁ ($\hat{\beta}_1$)			ISE($\hat{\beta}_2$)			$\sum_{j=3}^{10} \text{ISE}(\hat{\beta}_j)$		
		0.5	5	20	0.5	5	20	0.5	5	20	0.5	5	20	0.5	5	20
3e-6	500	38.38	25.27	25.00	155.59	82.91	36.46	164.92	93.57	99.40	164.71	100.38	88.51	642.11	2.16	0.00
	1000	37.21	25.13	25.13	176.36	65.40	8.29	186.25	95.80	119.49	186.53	99.60	91.30	552.30	0.26	0.00
	2500	125.31	25.35	36.39	488.35	15.22	0.01	544.88	129.07	854.95	590.05	104.22	171.14	5299.06	0.00	0.00
7e-6	500	32.74	24.68	24.63	121.04	65.59	24.82	126.28	76.51	90.90	123.97	80.76	75.05	380.57	1.88	0.00
	1000	29.46	24.55	24.92	124.44	46.78	3.17	131.87	78.13	119.20	129.41	80.36	76.49	192.16	0.07	0.00
	2500	33.77	24.91	38.03	130.76	225	0.00	173.80	119.71	971.82	166.64	84.10	170.07	423.71	0.00	0.00
5e-5	500	26.25	23.85	24.68	69.55	43.72	24.65	74.02	57.00	110.95	67.35	51.13	61.40	106.49	0.32	0.00
	1000	24.78	23.73	24.96	61.06	22.02	5.11	73.90	58.95	135.54	67.83	51.70	63.14	24.35	0.00	0.00
	2500	24.27	24.83	43.65	24.33	1.52	0.00	77.49	138.32	1358.97	69.31	59.66	175.91	1.50	0.00	0.00
2e-4	500	24.94	24.21	26.50	58.75	53.64	67.63	74.63	87.52	203.36	51.49	48.19	87.87	49.83	0.18	0.00
	1000	24.20	24.14	26.36	50.60	40.02	34.84	75.56	88.23	204.51	52.41	49.09	90.85	6.57	0.00	0.00
	2500	23.99	24.27	37.26	19.63	5.92	0.29	79.92	106.17	923.68	54.38	54.13	155.49	0.00	0.00	0.00

Table 1: The performance of the FadDoS estimator with varying tuning parameters is evaluated by PMSE of 1000 test samples and ISE of corresponding estimated coefficient functions. Each entry of PMSE is the average of 100 simulation replicates. The training sample size is $n = 200$.

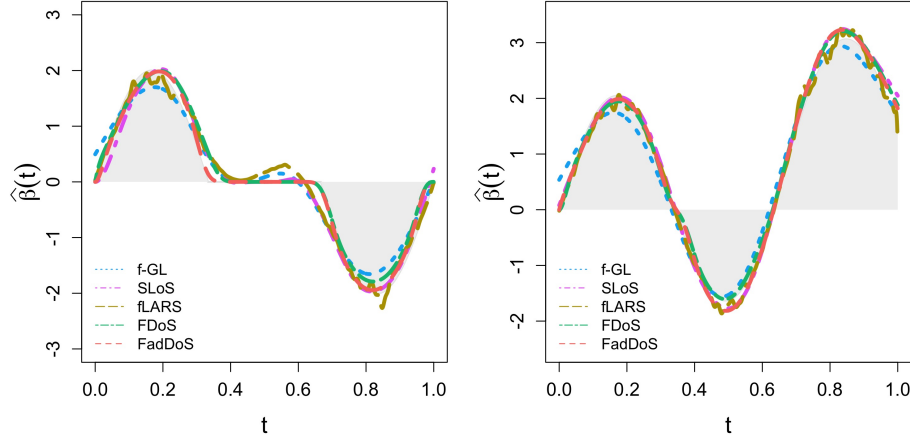


Figure 3: Comparison of estimated coefficient functions for $\hat{\beta}_1(t)$ (left panel) and $\hat{\beta}_2(t)$ (right panel) using f-GL (Gertheiss et al., 2013), SLoS (Lin et al., 2017), fLARS (Cheng et al., 2020), FDoS, and FadDoS. The shaded grey areas denote the true functions. The sample size is $n = 200$.

addressed by the functional SCAD penalty of the SLoS estimator. Note that the use of proper adaptive weights in the FadDoS estimator can lead to more accurate estimation of zero and nonzero regions of $\beta_1(t)$ and $\beta_2(t)$ simultaneously, and at the same time reduce the number of false negatives, namely avoiding nonzero estimates of true zero functions. It can be seen that, when the sample size is relatively small, the nonadaptive FDoS estimator has the smallest error in the zero subregion. This is likely due to the same degrees of regularization set for all functional covariates and heavy penalization is applied to identify all-zero covariates. The average TNR of the eight zero coefficients functions $\beta_j(t)$, $j = 3, \dots, 10$ are also presented in Table 2. Globally sparse

	Methods	PMSE($\times 10^{-3}$)	ISE ₀ ($\hat{\beta}_1$)	ISE ₁ ($\hat{\beta}_1$)	ISE($\hat{\beta}_2$)	$\sum_{j=3}^{10}$ ISE($\hat{\beta}_j$)	avgTNR
n=100	f-GL	28.98(3.10)	73.37(60.60)	271.32(130.99)	291.61(188.69)	45.89(46.13)	0.43(0.05)
	SLoS	27.73(3.73)	44.97(67.95)	180.45(157.71)	128.05(63.48)	49.79(97.26)	0.87(0.22)
	fLARS	33.74(3.03)	77.50(64.47)	164.04(88.11)	142.65(62.39)	106.35(113.63)	0.39(0.05)
	FDoS	28.53(3.16)	41.71(62.05)	187.11(97.53)	147.51(76.02)	72.16(57.01)	0.57(0.03)
	FadDoS	25.88(2.26)	44.55(67.87)	137.50(77.03)	107.87(49.02)	4.20(18.91)	0.99(0.01)
n=200	f-GL	25.17(1.76)	61.61(40.15)	181.39(92.06)	225.18(162.19)	21.04(19.32)	0.40(0.04)
	SLoS	24.50(1.94)	30.05(27.70)	79.53(37.25)	62.87(41.56)	11.39(39.47)	0.92(0.17)
	fLARS	30.52(2.00)	52.92(39.43)	78.00(45.02)	64.28(31.34)	48.73(51.99)	0.36(0.05)
	FDoS	24.29(1.74)	13.80(23.48)	69.59(36.44)	57.25(36.44)	23.19(29.16)	0.80(0.04)
	FadDoS	23.57(1.53)	18.27(28.47)	54.23(30.40)	49.11(25.14)	0.00(0.00)	1.00(0.00)
n=300	f-GL	24.12(1.66)	46.90(28.63)	155.68(85.30)	195.43(151.44)	13.96(11.61)	0.39(0.04)
	SLoS	23.67(1.66)	22.27(16.80)	63.33(31.59)	45.10(20.46)	4.21(16.24)	0.94(0.12)
	fLARS	29.59(1.84)	32.36(17.12)	57.28(32.22)	45.69(20.05)	31.98(17.12)	0.39(0.04)
	FDoS	23.37(1.66)	8.00(11.18)	47.21(26.57)	38.34(17.14)	15.21(19.69)	0.82(0.02)
	FadDoS	23.04(1.59)	7.64(13.39)	42.31(23.50)	35.40(16.16)	0.00(0.00)	1.00(0.00)

Table 2: PMSE, ISE, and average TNR (avgTNR) of the proposed estimators FDoS and FadDoS as well as f-GL (Gertheiss et al., 2013), SLoS (Lin et al., 2017), and fLARS (Cheng et al., 2020). The entry in the parenthesis for PMSE and ISE corresponds to the standard deviation among 100 simulation replicates, while the entry for avgTNR corresponds to the standard deviation among X_j , $j = 3, \dots, 10$.

estimators f-GL and fLARS are still inferior to the others probably due to the complex coefficient function setting containing zero subregions and zero-crossing. It is noteworthy that FadDoS slightly outperforms SLoS. One explanation is that the penalization terms in FadDoS are weighted by the initial functional coefficient estimates to control both global and local sparsity, while the sparsity parameters for every functional covariate designed in SLoS are identical. Therefore, the SLoS estimator might not well regularize both global and local shrinkage simultaneously. Another observation of SLoS is the larger variation of average TNR compared to FDoS or FadDoS, which is because of the worse estimation at the last coefficient function. It is admitted that tail fluctuation is usual when using polynomial splines. Nevertheless, the improved estimation of FDoS or FadDoS is possible because the roughness penalty is embedded in the functional $\ell_{1,2}$ penalty term rather than placed independently so that the wiggleness issue is alleviated.

5 Application

In this section, the new method is applied to the motivating Kinect study to examine the association between elderly mobility assessments and their multi-joint movements. A total of 50 subjects

aged between 68 and 89 years from four Neighbourhood Elderly Centres (NECs) in Hong Kong participated in the study. The participants performed a functional balance test called Timed Up and Go (TUG) test (Podsiadlo and Richardson, 1991), during which Kinect sensor monitored the three-dimensional displacements of 25 skeletal joints. The whole process of TUG test includes standing up from the chair, walking forward, turning around, walking back to the chair, and sitting down, as illustrated in Figure S2. We use their Balance Evaluation Systems Test (BESTest) scores as the measure of general functional balance and walking capability (Horak et al., 2009). In the pre-processing step, since the shorter completion time itself reflects better mobility (Nielsen et al., 2016), we padded the shorter signals till all observations have an equal time length to preserve a series of sequential raw actions, instead of warping time to align all movement signals. Additionally, all displacement signals are interpolated to ensure the same sampling rate. We calculate velocity by taking the first derivative of displacement signals. It is prioritized over displacement because they are less likely to be affected by different positioning of the Kinect sensor. In addition, previous research has shown interesting frequency patterns during walking (Kestenbaum et al., 2015; Morgan and Noehren, 2018), and therefore we include frequency domain knowledge to provide a more insightful understanding of joint movement patterns for the entire activity. The frequency domain information is obtained via Fourier transform. In scalar-on-function regression model, we regress the average BESTtest score on three-dimensional velocity and frequency domain data respectively in order to identify associated joints and investigate in detail how joint movements are associated with mobility assessments over the time and frequency domains.

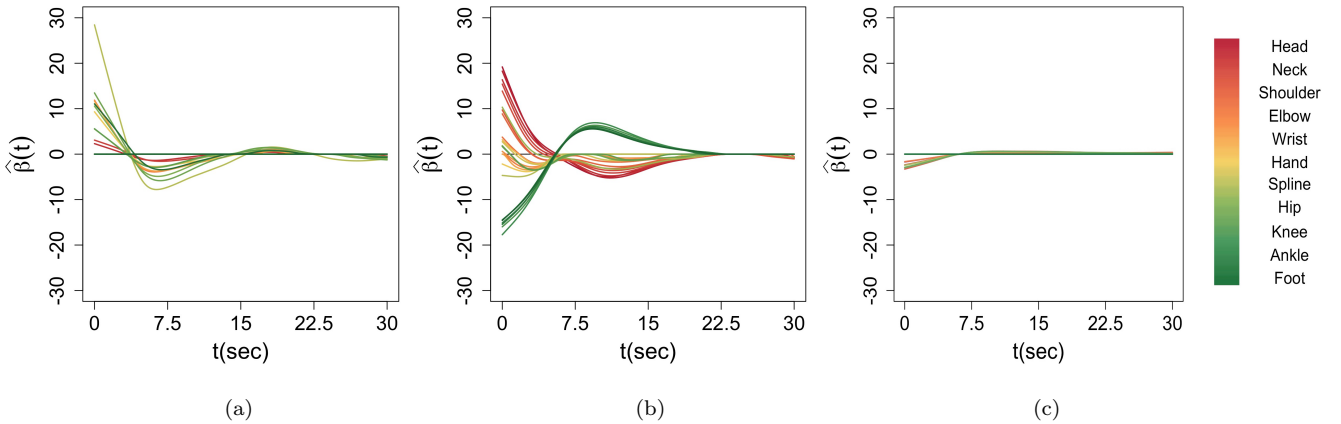


Figure 4: The estimated coefficient functions of (a) horizontal velocity, (b) vertical velocity, and (c) walking velocity. Each curve represents the estimated coefficient function of a joint and is color coded as Figure 1(b).

Figure 4(a) shows that the horizontal velocity of all joints shares an almost identical pace and therefore yields similar estimates. The estimates are positive till around 3 seconds when the healthy elderly stand up, which implies that faster ascending comes with good mobility. All estimates are close to zero around 18 seconds when the majority of the subjects finished the test. Figure 4(b) exhibits three clusters of behavior patterns related to joints in head, trunk and upper limbs, and lower limbs. The positive coefficients for the upward velocity from head to shoulder in the beginning also reveal that the swifter standing up the better mobility. Due to the setup of the sensor shown in Figure 1(a), the trunk and upper limbs are closer to the position of the Kinect camera, namely the origin of the three-dimensional coordinates, leading to relatively weaker effects. For lower limbs, high velocity during ascending and walking forward implies good physical capability. Moreover, the direction of vertical velocity is reversed when walking backward. It is reflected in the change of the signs in the estimates, all of which cross zero around 7 seconds as the healthy elderly turn. It is observed that the amplitude of the estimated coefficient is maximized at 12 seconds for head or 10 seconds for lower limbs when returning to the chair. The lag is due to the downward motion of head during sitting down. The nonzero estimates of most joints depicted in Figure 4(c) display consistent patterns. Since the stride velocity during walking forward is negative due to the Kinect camera setup, negative estimates before 7 seconds also indicate the faster pace the better mobility assessment.

Figure 5 exhibits the estimated coefficient functions in the frequency spectrum from 0 Hz to 17 Hz along three directions. Figure 5(a) demonstrates that only joints of shoulder, elbows, and

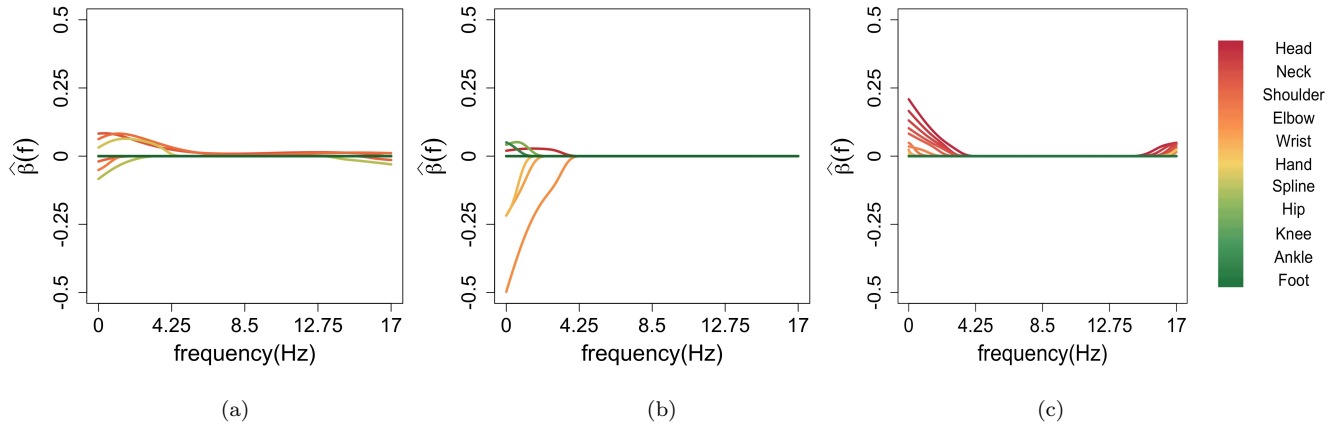


Figure 5: The estimated coefficient functions of (a) horizontal frequency, (b) vertical frequency, and (c) walking frequency. Each curve represents the estimated coefficient function of a joint and is color coded as Figure 1(b).

hands have substantial nonzero effects in part of the horizontal frequency domain, where the low-frequency oscillation reflects the arm’s horizontal swinging motion during walking, while the high-frequency oscillation represents the horizontally involuntary and rhythmic shaking probably caused by some disorders, thus associated with lower mobility (Hess and Pullman, 2012). The estimates of vertical oscillations of the shoulder, spine, and ankles are positive only at low frequencies as shown in Figure 5(b), representing the natural up-and-down oscillation in the normal stride. However, the negative estimates imply that the vertical swinging movement of hands is generally seen among the low-mobility elderly who spend excessive energy vertically to assist with walking. Additionally, Figure 5(c) shows that only joints between head and hands in the walking direction are associated with mobility. The nonzero estimates at the low-frequency domain confirm that the average stride frequency is 2 Hz (Henriksen et al., 2004). The magnitude of the effect decreases from the top joints to the bottom is likely because intensive head motions tilting forward are compensatory for trunk pitch to stabilize the body (Hirasaki et al., 1993, 1999). Moreover, the positive estimates of high-frequency oscillation are probably due to normal action tremors present in healthy individuals for active movements (Hess and Pullman, 2012).

6 Conclusion

While scalar-on-function regression model is appealing for multi-dimensional sensor data, where a large number of functional covariates are collected and scalar responses are measured, the double-sparsity property is critical for the interpretability of the model. Thus, we propose the novel FadDoS estimator, based on which we develop a nice double-sparsity model. In particular, one can concurrently identify important functional covariates and influential nonzero subregions throughout the entire domain. Our estimator is developed based on the new functional generalization of sparse group lasso to control local and global sparsity respectively, as well as smoothness. We further enhance it with adaptation where the penalty can be weighted by preliminary estimates. The FadDoS estimator enjoys the oracle property under mild conditions of the initial estimator and therefore it is theoretically sounder than the nonadaptive version. Simulation studies also show that our estimator outperforms existing methods with optimal performance.

Our work has provided an effective method for analyzing wearable sensor data, especially those that capture high-dimensional functional signals. In the application of Kinect sensor study, we

achieved satisfactory performance and identified the associated joints and their detailed association over both time and frequency domains. However, the FadDoS estimator is more general than this, as it is also applicable to other types of sensor devices that collect multi-dimensional signals including acceleration, heart rates, skin impedance, and more, thus promoting the use of advanced sensor devices in health research and having wider applications in the health field.

Acknowledgments

The authors thank all participants who took part in the study and the researchers who assisted with data collection.

Funding

This study was supported by the City University of Hong Kong internal research grant No.9610473.

References

- Beer, C., Aizenstein, J., Anderson, J., and Krafty, T. (2019). Incorporating prior information with fused sparse group lasso: Application to prediction of clinical measures from neuroimages. *Biometrics*, 75:1299–1309.
- Boyd, S., Parikh, N., Chu, E., Peleato, B., and Eckstein, J. (2010). Distributed optimization and statistical learning via the alternating direction method of multipliers. *Foundations and Trends in Machine Learning*, 3:1–122.
- Cardot, H., Ferraty, F., and Sarda, P. (2003). Spline estimators for the functional linear model. *Statistica Sinica*, 13:571–791.
- Cheng, Y., Shi, J., and Eyre, J. (2020). Nonlinear mixed-effects scalar-on-function models and variable selection. *Statistics and Computing*, 30:129–140.
- Cippitelli, E., Gasparrini, S., Spinsante, S., and Gambi, E. (2015). Kinect as a tool for gait analysis: Validation of a real time joints extraction algorithm working in side view. *Sensors*, 15:1417–1434.
- Collazos, A., Dias, R., and Zambom, Z. (2016). Consistent variable selection for functional regression models. *Journal of Multivariate Analysis*, 146:63–71.

- De Boor, C. (2001). *A Practical Guide to Splines*. Springer.
- Fan, J. and Li, R. (2001). Variable selection via nonconcave penalized likelihood and its oracle properties. *Journal of the American Statistical Association*, 96:1348–1360.
- Friedman, J., Hastie, T., and Tibshirani, R. (2010). A note on the group lasso and a sparse group lasso. *arXiv:1001.0736*.
- Gasparrini, S., Cippitelli, E., Spinsante, S., and Gambi, E. (2014). A depth-based fall detection system using a kinect sensor. *Sensors*, 14(2):2756–2775.
- Gertheiss, J., Maity, A., and Staicu, A. (2013). Variable selection in generalized functional linear models. *Stat*, 2:86–101.
- Henriksen, M., Lund, H., Moe-Nilssen, R., Bliddal, H., and Danneskiold-Samsøe, B. (2004). Test-retest reliability of trunk accelerometric gait analysis. *Gait & Posture*, 19(3):288–297.
- Hess, C. W. and Pullman, S. L. (2012). Tremor: Clinical phenomenology and assessment techniques. *Tremor and other Hyperkinetic Movements (New York, N.Y.)*, 2:tre-02-65-365-1.
- Hirasaki, E., Kubo, T., Nozawa, S., Matano, S., and Matsunaga, T. (1993). Analysis of head and body movements of elderly people during locomotion. *Acta oto-laryngologica. Supplementum*, 501:25–30.
- Hirasaki, E., Moore, S. T., Raphan, T., and Cohen, B. (1999). Effects of walking velocity on vertical head and body movements during locomotion. *Experimental brain research*, 127(2):117–130.
- Horak, F. B., Wrisley, D. M., and Frank, J. (2009). The balance evaluation systems test (bestest) to differentiate balance deficits. *Physical Therapy*, 89(5):484–498.
- Huang, J., Ma, S., Xie, H., and Zhang, C.-H. (2009). A group bridge approach for variable selection. *Biometrika*, 68:339–355.
- James, G., Wang, J., Zhu, J., and et al. (2009). Functional linear regression that’s interpretable. *The Annals of Statistics*, 37(5A):2083–2108.

- Kestenbaum, M., Michalec, M., Yu, Q., Pullman, S. L., and Louis, E. D. (2015). Intention tremor of the legs in essential tremor: Prevalence and clinical correlates. *Movement Disorders Clinical Practice*, 2(1):24–28.
- Kohout, J., Verešpejová, L., Kříž, P., Červená, L., Štícha, K., Crha, J., Trnková, K., Chovanec, M., and Mareš, J. (2021). Advanced statistical analysis of 3d kinect data: Mimetic muscle rehabilitation following head and neck surgeries causing facial paresis. *Sensors*, 21(1):103.
- Li, X., Mo, L., Yuan, X., and Zhang, J. (2014). Linearized alternating direction method of multipliers for sparse group and fused lasso models. *Computational Statistics & Data Analysis*, 79:203–221.
- Lin, Z., Cao, J., Wang, L., and et al. (2017). Locally sparse estimator for functional linear regression models. *Journal of Computational and Graphical Statistics*, 26(2):306–318.
- Matsui, H. and Konishi, S. (2011). Variable selection for functional regression models via the l_1 regularization. *Computational Statistics & Data Analysis*, 55(1):3304–3310.
- Meier, L., Van de Geer, S., and Bühlmann, P. (2009). High-dimensional additive modeling. *The Annals of Statistics*, 37:3779–3821.
- Mingotti, N., Lillo, R., and Romo, J. (2013). Lasso variable selection in functional regression. *Statistics and Econometrics*, Working paper:13–14.
- Morgan, K. and Noehren, B. (2018). Identification of knee gait waveform pattern alterations in individuals with patellofemoral pain using fast fourier transform. *PLoS ONE*, 13(12):e0209015.
- Nielsen, L., Kirkegaard, H., Østergaard, L., and et al. (2016). Comparison of self-reported and performance-based measures of functional ability in elderly patients in an emergency department: implications for selection of clinical outcome measures. *BMC Geriatrics*, 16:199.
- Pannu, J. and Billor, N. (2017). Robust group-lasso for functional regression model. *Communications in Statistics - Simulation and Computation*, 46(5):3356–3374.
- Park, J., Anh, J., and Jeon, Y. (2022). Sparse functional linear discriminant analysis. *Biometrika*, 109(1):209–226.

- Podsiadlo, D. and Richardson, S. (1991). The timed ‘up & go’: a test of basic functional mobility for frail elderly persons. *Journal of the American Geriatrics Society*, 39:142–148.
- Poignard, B. (2018). Asymptotic theory of the adaptive sparse group lasso. *Annals of the Institute of Statistical Mathematics*, 72:297–328.
- Ramsay, J. and Silverman, B. (2005). *Functional Data Analysis*. Springer.
- Simon, N., Friedman, J., Hastie, T., and Tibshirani, R. (2013). A sparse-group lasso. *Journal of Computational and Graphical Statistics*, 22(2):231–245.
- Tu, C. Y., Park, J., and Wang, H. (2020). Estimation of functional sparsity in nonparametric varying coefficient models for longitudinal data analysis. *Statistica Sinica*, 30:439–465.
- Tu, C. Y., Song, D., Breidt, F. J., Berger, T., and Wang, H. (2012). Functional model selection for sparse binary time series with multiple inputs. *Economic Time Series: Modeling and Seasonality*, page 477–497.
- Wang, H. and Kai, B. (2015). Functional sparsity: Global versus local. *Statistica Sinica*, 25:1337–1354.
- Wang, X. and Yuan, X. (2012). The linearized alternating direction method for dantzig selector. *SIAM Journal on Scientific Computing*, 34:A2792–A2811.
- Zhou, J., Wang, N., and Wang, N. (2013). Functional linear model with zero-value coefficient function at sub-regions. *Statistica Sinica*, 23(1):25–50.
- Zou, H. (2006). The adaptive lasso and its oracle properties. *Journal of the American Statistical Association*, 101:1418–1429.

Supplementary Material for “Functional Adaptive Double-Sparsity Estimator for Functional Linear Regression Model with Multiple Functional Covariates”

Cheng Cao

School of Data Science, City University of Hong Kong

Jiguo Cao

Department of Statistics and Actuarial Science, Simon Fraser University

Hailiang Wang

School of Design, The Hong Kong Polytechnic University

Kwok-Leung Tsui

Grado Department of Industrial and Systems Engineering,
Virginia Polytechnic Institute and State University

Xinyue Li

School of Data Science, City University of Hong Kong

July 13, 2023

This supplementary material includes illustrations of the simulation studies, real data application, and theoretical results of our proposed method. The figures to demonstrate simulation performance and Timed Up and Go test are shown in Section S1 and S2. We provide derivations of Alternating Direction Method of Multipliers (ADMM) subproblems in Section S3. The proofs of Theorem 1-Theorem 4 are given in Section S4.

1 Effects of the Tuning Parameters

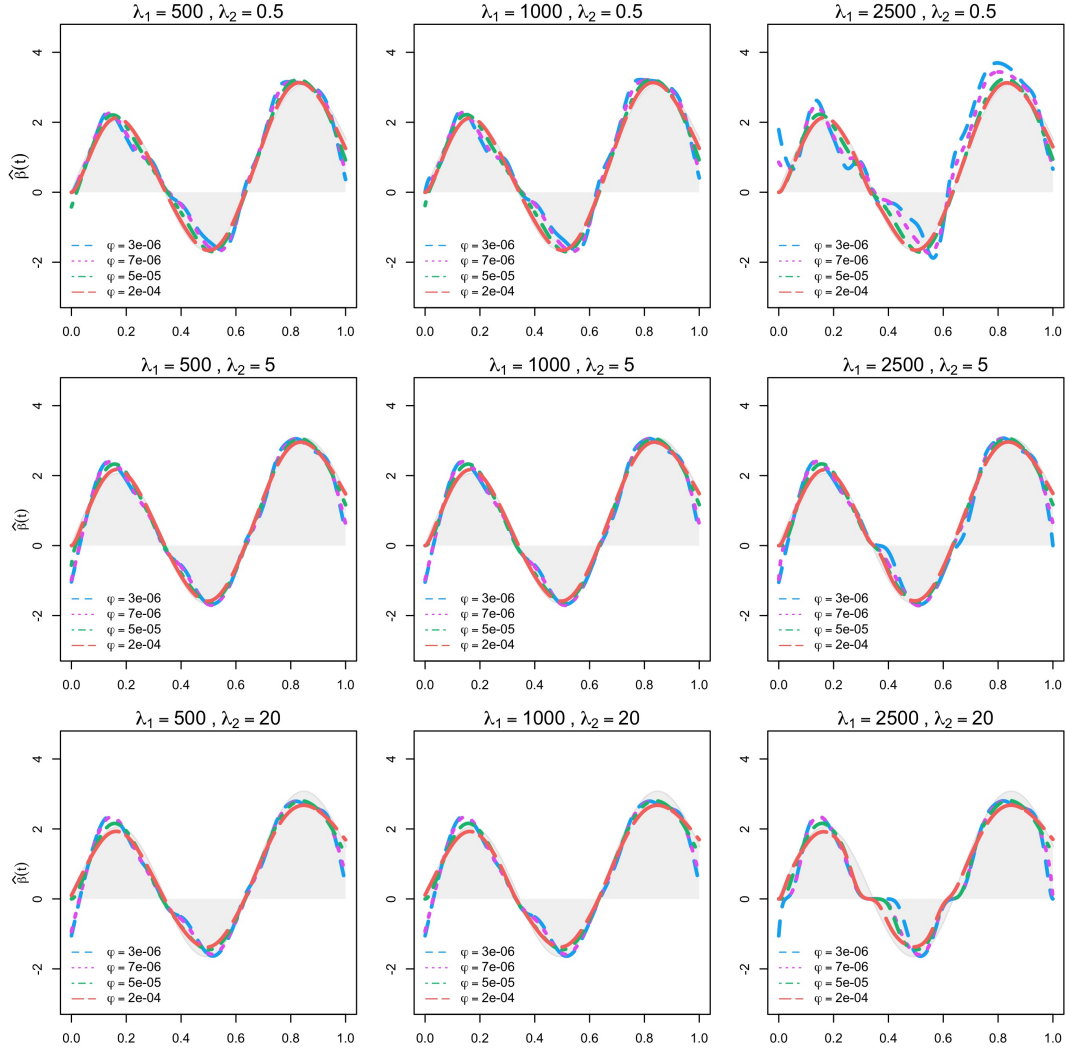
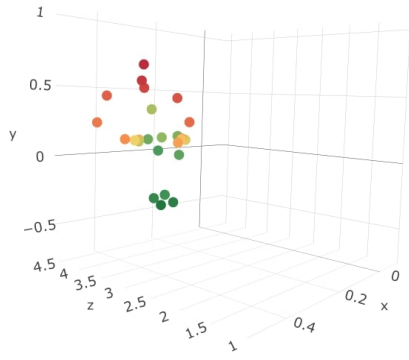
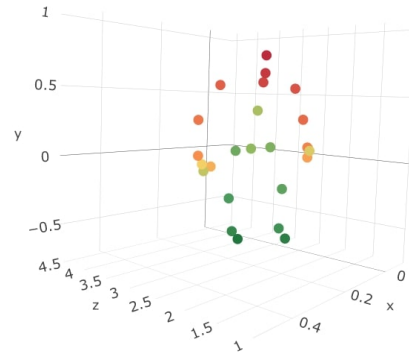


Figure S1: Estimated coefficient functions for $\beta_2(t)$ using FadDoS with varying tuning parameters. The sample size is $n = 200$.

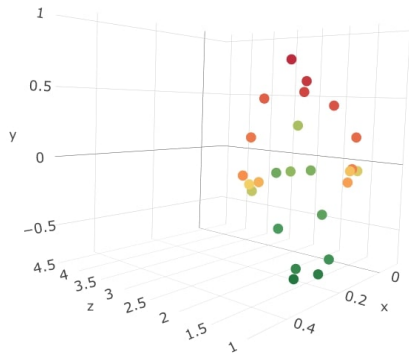
2 Timed Up and Go Test



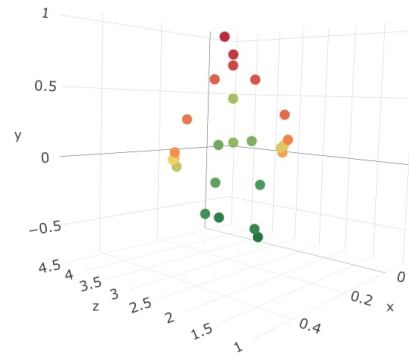
(a)



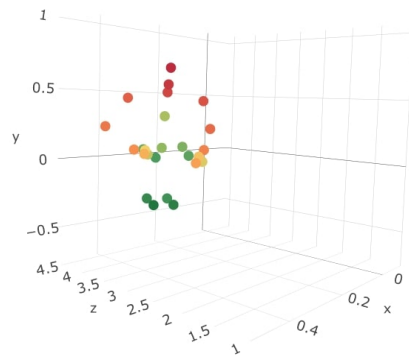
(b)



(c)



(d)



(e)

Figure S2: Instruction of Timed Up and Go (TUG) Test : (a) Stand up from the chair; (b) Walk forward at a normal pace; (c) Turn; (d) Walk backward to the chair at a normal pace; (e) Sit down. Each joint is color coded as Figure 1(b).

3 Derivation of ADMM subproblems

3.1 Solution to $\tilde{\mathbf{b}}$ -update

Based on the Equation (8),

$$\begin{aligned}
\tilde{\mathbf{b}}_l^{k+1} &= \arg \min_{\tilde{\mathbf{b}}_l \in \mathbb{R}^{M_n+d}} \frac{1}{2} \|\mathbf{r}_{(-l)} - \tilde{\mathbf{U}}_l \tilde{\mathbf{b}}_l\|_2^2 + \lambda_2 \|\tilde{\mathbf{b}}_l\|_2 + (\mathbf{u}_l^k)^T ((\mathbf{L}_l^T)^{-1} \tilde{\mathbf{b}}_l - \mathbf{z}_l^k) + \frac{\rho}{2} \|(\mathbf{L}_l^T)^{-1} \tilde{\mathbf{b}}_l - \mathbf{z}_l^k\|_2^2 \\
&= \arg \min_{\tilde{\mathbf{b}}_l \in \mathbb{R}^{M_n+d}} \frac{1}{2} \|\mathbf{r}_{(-l)} - \tilde{\mathbf{U}}_l \tilde{\mathbf{b}}_l\|_2^2 + \lambda_2 \|\tilde{\mathbf{b}}_l\|_2 + \frac{\rho}{2} \|(\mathbf{L}_l^T)^{-1} \tilde{\mathbf{b}}_l - \mathbf{z}_l^k - \mathbf{u}_l^k / \rho\|_2^2 \\
&= \arg \min_{\tilde{\mathbf{b}}_l \in \mathbb{R}^{M_n+d}} \lambda_2 \|\tilde{\mathbf{b}}_l\|_2 + \frac{1}{2} \|\hat{\mathbf{r}}_{(-l)}^k - \hat{\mathbf{U}}_l \tilde{\mathbf{b}}_l\|_2^2,
\end{aligned}$$

where $\hat{\mathbf{U}}_l = (\tilde{\mathbf{U}}_l^T, \sqrt{\rho} \mathbf{L}_l^{-1})^T$ and $\hat{\mathbf{r}}_{(-l)}^k = (\mathbf{r}_{(-l)}^T, \sqrt{\rho}(\mathbf{z}_l^k + \mathbf{u}_l^k / \rho))^T$. Since $\hat{\mathbf{U}}_l$ is not identity, we cannot directly get the solution to the second operator. Fortunately, by following Wang and Yuan (2012) we can employ linearization technique to approximate the quadratic term efficiently. We linearize it by replacing $\|\hat{\mathbf{r}}_{(-l)}^k - \hat{\mathbf{U}}_l \tilde{\mathbf{b}}_l\|_2^2 / 2$ with $(\hat{\mathbf{U}}_l^T (\hat{\mathbf{U}}_l \tilde{\mathbf{b}}_l^k - \hat{\mathbf{r}}_{(-l)}^k))^T (\tilde{\mathbf{b}}_l - \tilde{\mathbf{b}}_l^k) + \frac{\nu_l}{2} \|\tilde{\mathbf{b}}_l - \tilde{\mathbf{b}}_l^k\|_2^2$, where the first term is apparently the gradient at $\tilde{\mathbf{b}}_l^k$. Hence,

$$\begin{aligned}
\tilde{\mathbf{b}}_l^{k+1} &= \arg \min_{\tilde{\mathbf{b}}_l \in \mathbb{R}^{M_n+d}} \lambda_2 \|\tilde{\mathbf{b}}_l\|_2 + (\hat{\mathbf{U}}_l^T (\hat{\mathbf{U}}_l \tilde{\mathbf{b}}_l^k - \hat{\mathbf{r}}_{(-l)}^k))^T (\tilde{\mathbf{b}}_l - \tilde{\mathbf{b}}_l^k) + \frac{\nu_l}{2} \|\tilde{\mathbf{b}}_l - \tilde{\mathbf{b}}_l^k\|_2^2 \\
&= \arg \min_{\tilde{\mathbf{b}}_l \in \mathbb{R}^{M_n+d}} \lambda_2 \|\tilde{\mathbf{b}}_l\|_2 + \frac{\nu_l}{2} \|\tilde{\mathbf{b}}_l - \tilde{\mathbf{b}}_l^k + \hat{\mathbf{U}}_l^T (\hat{\mathbf{U}}_l \tilde{\mathbf{b}}_l^k - \hat{\mathbf{r}}_{(-l)}^k) / \nu_l\|_2^2 \\
&= S_{2, \lambda_2 / \nu_l}(\tilde{\mathbf{b}}_l^k - \hat{\mathbf{U}}_l^T (\hat{\mathbf{U}}_l \tilde{\mathbf{b}}_l^k - \hat{\mathbf{r}}_{(-l)}^k) / \nu_l).
\end{aligned}$$

If ρ is fixed, $\tilde{\mathbf{b}}_l^{k+1}$ will tend to be zero when $\lambda_2 \geq \nu_l \|\tilde{\mathbf{b}}_l^k - \hat{\mathbf{U}}_l^T (\hat{\mathbf{U}}_l \tilde{\mathbf{b}}_l^k - \hat{\mathbf{r}}_{(-l)}^k) / \nu_l\|_2$.

3.2 Solution to \mathbf{z} -update

Based on the Equation (9),

$$\begin{aligned}
\mathbf{z}^{k+1} &= \arg \min_{\mathbf{z} \in \mathbb{R}^{J \times (M_n+d)}} \lambda_1 \|\mathbf{z}\|_1 + (\mathbf{u}^k)^T (\mathbf{D} \tilde{\mathbf{b}}^{k+1} - \mathbf{z}) + \frac{\rho}{2} \|\mathbf{D} \tilde{\mathbf{b}}^{k+1} - \mathbf{z}\|_2^2 \\
&= \arg \min_{\mathbf{z} \in \mathbb{R}^{J \times (M_n+d)}} \lambda_1 \|\mathbf{z}\|_1 + \frac{\rho}{2} \|\mathbf{D} \tilde{\mathbf{b}}^{k+1} - \mathbf{z} + \mathbf{u}^k / \rho\|_2^2 \\
&= S_{1, \lambda_1 / \rho}(\mathbf{D} \tilde{\mathbf{b}}^{k+1} + \mathbf{u}^k / \rho).
\end{aligned}$$

If ρ is fixed, z_r^{k+1} will tend to be zero when $\lambda_1 > |\rho \mathbf{D}_{r\cdot}^T \tilde{\mathbf{b}}^{k+1} + u_r^k|$, $r = 1, \dots, J \times (M_n + d)$, where $\mathbf{D}_{r\cdot}$ is the r th row of \mathbf{D} .

4 Proofs

B-spline is essential in the estimation of coefficient function for functional model. Before presenting the proofs of the proposed estimator, it is necessary to state some properties of B-splines. As mentioned in Section 2.2, B-splines have a local support property: at most $d+1$ consecutive subintervals are nonzero. Plus, for a collection of B-spline basis functions $\{B_k(t) : k = 1, \dots, M_n + d, t \in \mathcal{T}\}$, $B_k(t) \geq 0$ and $\sum_{k=1}^{M_n+d} B_k(t) = 1$ for all t . These properties imply that

$$\sup_{k,r} |\langle B_k, B_r \rangle| \leq 2(d+1)M_n^{-1}, \quad (\text{S1})$$

and thus,

$$\|B_k\|_2^2 \leq \sup_{k,r} |\langle B_k, B_r \rangle| \leq 2(d+1)M_n^{-1}. \quad (\text{S2})$$

In addition, three inequalities will be also used. For any $x \in \mathbb{R}^p$

$$\begin{aligned} \|x\|_2 &\leq \|x\|_1 \leq \sqrt{p}\|x\|_2; \\ \|x\|_\infty &\leq \|x\|_1 \leq p\|x\|_\infty; \\ \|x\|_\infty &\leq \|x\|_2 \leq \sqrt{p}\|x\|_\infty. \end{aligned}$$

The following Lemma 1 can be found in Theorem XII(6) of De Boor (2001), illustrating the convergence of the B-spline approximant.

Lemma 1. *there exists $\beta_\alpha(t)$ such that $\|\beta - \beta_\alpha\|_\infty \leq C_1 M_n^{-\delta}$ for some constant $C_1 \geq 0$, where $\beta_\alpha(t) \stackrel{\text{def}}{=} \mathbf{B}(t)^T \boldsymbol{\alpha}$.*

4.1 Proof of Theorem 1

The proof requires Lemma 2, which is followed from Huang et al. (2004) Lemma A.3. The lemma is the same as A_8 in Zhou et al. (2013) and (C4) in Lin et al. (2017), who defined the covariance operator of the random process $X(t)$ in their notations.

Lemma 2. *If $\lim_{n \rightarrow \infty} M_n \log M_n / n = 0$, there are positive constants C_2 and C_3 such that, all eigenvalues of $(M_n/n)\mathbf{U}^T\mathbf{U}$ are within the interval $[C_2, C_3]$ with probability tending to 1 as $n \rightarrow \infty$.*

Lemma 3. *There are positive constants C_4 and C_5 such that, all eigenvalues of $\mathbf{K}_{\varphi,l}$ are within the interval $[C_4\varphi M_n^{-1}, C_5 M_n^{-1}]$.*

Proof. We define $\mathbf{K}_{\varphi,l} = \mathbf{\Phi}_l + \varphi\mathbf{\Omega}_l$, where $(\mathbf{\Phi}_l)_{pq} = \int_t B_{lp}(t)B_{lq}(t)dt$ and $(\mathbf{\Omega}_l)_{pq} = \int_t B_{lp}^m(t)B_{lq}^m(t)dt$. The proof follows Lemma 6.2 (i) in Cardot et al. (2003).

For simplicity of notation, we assume the model has no intercept, i.e., $\boldsymbol{\mu} = \mathbf{0}$ and rewrite the objective in Equation (2.5)

$$L_n(\mathbf{b}) = \frac{1}{n} \|\mathbf{Y} - \mathbf{U}\mathbf{b}\|_2^2 + \Delta_n \lambda_1 \sum_{l=1}^J w_l^{(1)} \|\mathbf{b}_l\|_1 + \lambda_2 \sum_{l=1}^J w_l^{(2)} (\mathbf{b}_l^T \mathbf{K}_{\varphi,l} \mathbf{b}_l)^{1/2}, \quad (\text{S3})$$

where $\mathbf{K}_{\varphi,l} = \mathbf{\Phi}_l + \varphi\mathbf{\Omega}_l$.

Let $D_n(\mathbf{v}) = L_n(\mathbf{b} + \eta_n \mathbf{v}) - L_n(\mathbf{b})$, where η_n is a scalar and $\mathbf{v} \in \mathbb{R}^{J \times (M_n + d)}$. At the point $\mathbf{b} = \boldsymbol{\alpha}$, we let $\hat{\mathbf{b}} = \boldsymbol{\alpha} + \eta_n \mathbf{v}$. By the minimality of $\hat{\mathbf{b}}$, we have

$$\begin{aligned} & \frac{1}{n} (\|\mathbf{Y} - \mathbf{U}(\boldsymbol{\alpha} + \eta_n \mathbf{v})\|_2^2 - \|\mathbf{Y} - \mathbf{U}\boldsymbol{\alpha}\|_2^2) \\ & \leq \Delta_n \lambda_1 \sum_{l \in \mathcal{A}} w_l^{(1)} (\|\boldsymbol{\alpha}_l\|_1 - \|\boldsymbol{\alpha}_l + \eta_n \mathbf{v}_l\|_1) + \lambda_2 \sum_{l \in \mathcal{A}} w_l^{(2)} ((\boldsymbol{\alpha}_l^T \mathbf{K}_{\varphi,l} \boldsymbol{\alpha}_l)^{1/2} - \\ & ((\boldsymbol{\alpha}_l + \eta_n \mathbf{v}_l)^T \mathbf{K}_{\varphi,l} (\boldsymbol{\alpha}_l + \eta_n \mathbf{v}_l))^{1/2}), \end{aligned} \quad (\text{S4})$$

because of the fact that $\boldsymbol{\alpha}_l = \mathbf{0}$ if $l \in \mathcal{A}^c$. Let $\epsilon_i = \mathbf{Y}_i - \langle \mathbf{X}_i, \boldsymbol{\beta} \rangle$, $\boldsymbol{\epsilon} = (\epsilon_1, \dots, \epsilon_n)$ and $e_i = \langle \mathbf{X}_i, \mathbf{B}^T \boldsymbol{\alpha} \rangle - \langle \mathbf{X}_i, \boldsymbol{\beta} \rangle = \langle \mathbf{X}_i, \boldsymbol{\beta}_\alpha - \boldsymbol{\beta} \rangle$, $\mathbf{e} = (e_1, \dots, e_n)$, the LHS of (S4) gives

$$\begin{aligned} \text{LHS} &= \frac{1}{n} \|\boldsymbol{\epsilon} - \mathbf{e} - \eta_n \mathbf{U}\mathbf{v}\|_2^2 - \frac{1}{n} \|\boldsymbol{\epsilon} - \mathbf{e}\|_2^2 \\ &= \frac{\eta_n^2}{n} \mathbf{v}^T \mathbf{U}^T \mathbf{U} \mathbf{v} - \frac{2\eta_n}{n} (\boldsymbol{\epsilon} - \mathbf{e})^T \mathbf{U} \mathbf{v}. \end{aligned}$$

By Lemma 2, $(\eta_n^2/n) \mathbf{v}^T \mathbf{U}^T \mathbf{U} \mathbf{v} \geq (\eta_n^2/n) \frac{C_{2n}}{M_n} = \eta_n^2 O_p(M_n^{-1})$, while by Cauchy-Schwarz inequality, $(2\eta_n/n) (\boldsymbol{\epsilon} - \mathbf{e})^T \mathbf{U} \mathbf{v} \leq (2\eta_n/n) \|\mathbf{v}\|_2 ((\boldsymbol{\epsilon} - \mathbf{e})^T \mathbf{U} \mathbf{U}^T (\boldsymbol{\epsilon} - \mathbf{e}))^{1/2}$. Since $\epsilon_i \stackrel{i.i.d}{\sim} N(0, \sigma^2)$, $\mathbb{E}[(\boldsymbol{\epsilon} - \mathbf{e})^T \mathbf{U} \mathbf{U}^T (\boldsymbol{\epsilon} - \mathbf{e})] = \mathbb{E}[\boldsymbol{\epsilon}^T \mathbf{U} \mathbf{U}^T \boldsymbol{\epsilon}] + \mathbb{E}[\mathbf{e}^T \mathbf{U} \mathbf{U}^T \mathbf{e}]$. By A.1, properties of B-splines and independence

of ϵ_i , we have

$$\begin{aligned}
\mathbb{E}[\boldsymbol{\epsilon}^T \mathbf{U} \mathbf{U}^T \boldsymbol{\epsilon}] &= \mathbb{E} \left[\sum_{l=1}^J \sum_{k=1}^{M_n+d} \left[\sum_{i=1}^n \langle X_{li}, B_{lk} \rangle^2 \epsilon_i^2 + \sum_{i' \neq i} \langle X_{li}, B_{lk} \rangle \langle X_{li'}, B_{lk} \rangle \epsilon_i \epsilon_{li'} \right] \right] \\
&\leq \sigma^2 \sum_{l=1}^J \sup_k \sum_{k=1}^{M_n+d} \sum_{i=1}^n |\langle X_{li}, B_{lk} \rangle|^2 \\
&\leq \sigma^2 J n \|X_{li}\|_2^2 \sup_k \sum_{r=1}^{M_n+d} |\langle B_{lr}, B_{lk} \rangle| \\
&= O(n M_n^{-1}).
\end{aligned}$$

On the other hand, by Cauchy-Schwarz inequality, A.1, and Lemma 1, $e_i^2 = |\langle \mathbf{X}_i, \boldsymbol{\beta}_\alpha - \boldsymbol{\beta} \rangle|^2 \leq \|\mathbf{X}_i\|_2^2 \sum_l \int_{\mathcal{T}} [\sup_t |\beta_{al}(t) - \beta_l(t)|]^2 dt \leq c_1^2 J |\mathcal{T}| (C_1 M_n^{-\delta})^2$, where $|\mathcal{T}|$ represents the length of time domain. The inequality still holds for $e_{il} e_{i'}$, $\forall i \neq i'$. Hence,

$$\begin{aligned}
\mathbb{E}[\mathbf{e}^T \mathbf{U} \mathbf{U}^T \mathbf{e}] &= \mathbb{E} \left[\sum_{l=1}^J \sum_{k=1}^{M_n+d} \left[\sum_{i=1}^n \langle X_{li}, B_{lk} \rangle^2 e_i^2 + \sum_{i' \neq i} \langle X_{li}, B_{lk} \rangle \langle X_{li'}, B_{lk} \rangle e_i e_{i'} \right] \right] \\
&\leq \sum_{k=1}^{M_n+d} \sum_{i=1}^n e_i^2 \mathbb{E}[\langle X_{li}, B_{lk} \rangle^2] + \sum_{k=1}^{M_n+d} \sum_{i' \neq i} e_i e_{i'} \mathbb{E}[\langle X_{li}, B_{lk} \rangle \langle X_{li'}, B_{lk} \rangle] \\
&= O(M_n^{-2\delta} n M_n^{-1}) + O(M_n^{-2\delta} n(n-1) M_n^{-1}) \\
&= O(n^2 M_n^{-2\delta-1}).
\end{aligned}$$

By A.3, we have $\mathbb{E}[\boldsymbol{\epsilon}^T \mathbf{U} \mathbf{U}^T \boldsymbol{\epsilon} + \mathbf{e}^T \mathbf{U} \mathbf{U}^T \mathbf{e}] = O(n M_n^{-1})$. By Markov inequality, $\boldsymbol{\epsilon}^T \mathbf{U} \mathbf{U}^T \boldsymbol{\epsilon} + \mathbf{e}^T \mathbf{U} \mathbf{U}^T \mathbf{e} = O_p(n M_n^{-1})$ and thus, $-(2\eta_n/n)(\boldsymbol{\epsilon} - \mathbf{e})^T \mathbf{U} \mathbf{v} \geq -2\eta_n \|\mathbf{v}\|_2 O_p(n^{-1/2} M_n^{-1/2})$. Therefore, the LHS gives

$$\text{LHS} \geq \eta_n^2 O_p(M_n^{-1}) - 2\eta_n O_p(n^{-1/2} M_n^{-1/2}) \|\mathbf{v}\|_2. \quad (\text{S5})$$

We denote the two terms of RHS of (S4) by T_1 and T_2 . We first show the convergence rate of FDoS by assuming $w_l^{(1)} = w_l^{(2)} = 1$ for all l . With triangle inequality and $\Delta_n = |\mathcal{T}|/M_n$, and let $|\mathcal{A}|$ be the number of nonzero functions,

$$\begin{aligned}
T_1 &\leq |\mathcal{T}| M_n^{-1} \lambda_1 \eta_n |\mathcal{A}| (J(M_n + d))^{1/2} \|\mathbf{v}\|_2 \\
&= \eta_n O_p(\lambda_1 M_n^{-1/2}) \|\mathbf{v}\|_2.
\end{aligned} \quad (\text{S6})$$

Let $g_{\mathbf{A}}(\mathbf{x}) = (\mathbf{x}^T \mathbf{A} \mathbf{x})^{1/2}$, we know that g is continuous function. By Taylor expansion and Lemma 3, $g_{\mathbf{K}_{\varphi,l}}(\boldsymbol{\alpha}_l) - g_{\mathbf{K}_{\varphi,l}}(\boldsymbol{\alpha}_l + \eta_n \mathbf{v}) \approx -\eta_n \mathbf{v}^T \nabla g_{\mathbf{K}_{\varphi,l}}(\boldsymbol{\alpha}_l)$ and with $\varphi = \lambda_2^2$, T_2 gives

$$\begin{aligned} T_2 &\leq -\lambda_2 |\mathcal{A}| \eta_n \|\mathbf{v}\|_2 (\boldsymbol{\alpha}_l^T \mathbf{K}_{\varphi,l} \boldsymbol{\alpha}_l)^{-1/2} \|\mathbf{K}_{\varphi,l} \boldsymbol{\alpha}_l\|_2 \\ &= \eta_n O_p(\lambda_2^2 M_n^{-1/2}) \|\mathbf{v}\|_2. \end{aligned} \tag{S7}$$

Combining three inequalities (S5)-(S7), we have

$$\eta_n^2 O_p(M_n^{-1}) - 2\eta_n O_p(n^{-1/2} M_n^{-1/2}) \|\mathbf{v}\|_2 \leq \eta_n O_p(\lambda_1 M_n^{-1/2}) \|\mathbf{v}\|_2 + \eta_n O_p(\lambda_2^2 M_n^{-1/2}) \|\mathbf{v}\|_2.$$

For sufficient large constant C_6 such that $\|\mathbf{v}\|_2 = C_6$, we find $\eta_n = O_p(M_n^{1/2} n^{-1/2} + M_n^{1/2} \lambda_1 + M_n^{1/2} \lambda_2^2)$. When $\lambda_1 = O(n^{-1/2})$ and $\lambda_2 = O(n^{-1/4})$, $\eta_n = O_p(M_n^{1/2} n^{-1/2})$. It means that for any given $\varepsilon > 0$, there always exists η_n such that

$$P\{\exists \mathbf{v} \in \mathbb{R}^{M_n+d}, \|\mathbf{v}\|_2 = C_6 : L_n(\boldsymbol{\alpha} + \eta_n \mathbf{v}) < L_n(\boldsymbol{\alpha})\} \geq 1 - \varepsilon.$$

This further means that there is a local minimizer $\hat{\mathbf{b}} = \boldsymbol{\alpha} + \eta_n \mathbf{v}$, such that $\|\hat{\mathbf{b}} - \boldsymbol{\alpha}\|_2 = O_p(M_n^{1/2} n^{-1/2})$.

Therefore, by triangle inequality

$$\begin{aligned} \|\hat{\boldsymbol{\beta}} - \boldsymbol{\beta}\|_{\infty} &\leq \|\hat{\boldsymbol{\beta}} - \boldsymbol{\beta}_{\alpha}\|_{\infty} + \|\boldsymbol{\beta}_{\alpha} - \boldsymbol{\beta}\|_{\infty} \\ &\leq \sup_t \sum_{k=1}^{M_n+d} |B_{lk}(t)| \|\hat{\mathbf{b}} - \boldsymbol{\alpha}\|_{\infty} + \|\boldsymbol{\beta}_{\alpha} - \boldsymbol{\beta}\|_{\infty} \\ &= O_p(M_n^{1/2} n^{-1/2}) + O(M_n^{-\delta}) \\ &= O_p(M_n^{1/2} n^{-1/2}). \end{aligned}$$

The last equation holds because of A.3.

The proof of convergence rate of FadDoS depends on the same reasoning before, except the step of T_1 and T_2 . Let $\phi_1 = \sup_{l \in \mathcal{A}} \|\check{\beta}_l\|_1^{-a}$ and $\phi_2 = \sup_{l \in \mathcal{A}} \|\check{\beta}_l\|_2^{-a}$. When $\lambda_1 \phi_1 = O(n^{-1/2})$ and $\lambda_2 \phi_2 = O(n^{-1/4})$, the results follow.

4.2 Proof of Theorem 2

Since the penalty terms of the objective function are separable, we assume other coefficient functions fixed and only consider the l th coefficient function here.

$$(n/M_n)^{1/2}(\hat{\beta}_l - \beta_l) = (n/M_n)^{1/2}(\hat{\beta}_l - \beta_{\alpha l}) + (n/M_n)^{1/2}(\beta_{\alpha l} - \beta_l).$$

The second term of RHS is the B-spline approximation error mentioned in Lemma 1, $(n/M_n)^{1/2}(\beta_{\alpha l} - \beta_l) = O(n^{1/2}M_n^{-\delta-1/2})$. Thus, we only need to focus on the first term of RHS, $(n/M_n)^{1/2}(\hat{\beta}_l - \beta_{\alpha l}) = (n/M_n)^{1/2}\mathbf{B}_l^T(\hat{\mathbf{b}}_l - \boldsymbol{\alpha}_l)$. Suppose that $\hat{\mathbf{b}}_l = \boldsymbol{\alpha}_l + (M_n/n)^{1/2}\mathbf{v}$, we define $\mathbf{r}_{(-l)} = \mathbf{Y} - \sum_{j \neq l} \mathbf{U}_j \mathbf{b}_j$, and then according to (S3)

$$\begin{aligned} Q(\mathbf{v}) = & \|\mathbf{r}_{(-l)} - \mathbf{U}_l(\boldsymbol{\alpha}_l + (M_n/n)^{1/2}\mathbf{v})\|_2^2 + \Delta_n \lambda_1 \|\boldsymbol{\alpha}_l + (M_n/n)^{1/2}\mathbf{v}\|_1 + \\ & \lambda_2 ((\boldsymbol{\alpha}_l + (M_n/n)^{1/2}\mathbf{v})^T \mathbf{K}_{\varphi,l}(\boldsymbol{\alpha}_l + (M_n/n)^{1/2}\mathbf{v}))^{1/2}. \end{aligned}$$

Suppose the minimizer of $Q(\mathbf{v})$ is noted as $\hat{\mathbf{v}}_n$, then $\hat{\mathbf{v}}_n = (n/M_n)^{1/2}(\hat{\mathbf{b}}_l - \boldsymbol{\alpha}_l)$. We need to show the limiting distribution of $\hat{\mathbf{v}}_n$ by proving the finite distribution convergence of $V_{1(n)}^{(l)}$ to $V_1^{(l)}$. Note that $V_{1(n)}^{(l)}(\mathbf{v}) = Q(\mathbf{v}) - Q(\mathbf{0})$,

$$\begin{aligned} V_{1(n)}^{(l)}(\mathbf{v}) = & [\mathbf{v}^T (\frac{M_n}{n} \mathbf{U}_l^T \mathbf{U}_l) \mathbf{v} - 2(\frac{M_n}{n})^{1/2}(\mathbf{r}_{(-l)} - \mathbf{U}_l \boldsymbol{\alpha}_l)^T \mathbf{U}_l \mathbf{v}] + \\ & \Delta_n \lambda_1 (\|\boldsymbol{\alpha}_l + (M_n/n)^{1/2}\mathbf{v}\|_1 - \|\boldsymbol{\alpha}_l\|_1) + \\ & \lambda_2 (((\boldsymbol{\alpha}_l + (M_n/n)^{1/2}\mathbf{v})^T \mathbf{K}_{\varphi,l}(\boldsymbol{\alpha}_l + (M_n/n)^{1/2}\mathbf{v}))^{1/2} - (\boldsymbol{\alpha}_l^T \mathbf{K}_{\varphi,l} \boldsymbol{\alpha}_l)^{1/2}). \end{aligned}$$

Let $(M_n/n)\mathbf{U}_l^T \mathbf{U}_l \rightarrow \mathbf{C}_l$ by Lemma 2 and $\mathbf{W}_l \sim N(\mathbf{0}, \sigma^2 \mathbf{C}_l)$, the first term denoted by T_1 of RHS of $V_{1(n)}^{(l)}(\mathbf{v})$ is

$$T_1 = \mathbf{v}^T \mathbf{C}_l \mathbf{v} - 2\mathbf{W}_l^T,$$

which is because that $(M_n/n)^{1/2}(\mathbf{r}_{(-l)} - \mathbf{U}_l \boldsymbol{\alpha}_l)^T \mathbf{U}_l = (M_n/n)^{1/2} \boldsymbol{\epsilon}^T \mathbf{U}_l + (M_n/n)^{1/2} \mathbf{e}^T \mathbf{U}_l$, and $(M_n/n)^{1/2} \boldsymbol{\epsilon}^T \mathbf{U}_l = \mathbf{W}_l$, $(M_n/n)^{1/2} \mathbf{e}^T \mathbf{U}_l = (M_n/n)^{1/2} O_p(M_n^{-\delta-1/2} n) = o_p(1)$. The second term denoted by T_2 of RHS of $V_{1(n)}^{(l)}(\mathbf{v})$ is

$$T_2 = \lambda_1 (nM_n)^{-1/2} \sum_{k=1}^{M_n+d} \left\{ |v_k| \mathbb{I}(\alpha_{lk} = 0) + v_k \text{sgn}(\alpha_{lk}) \mathbb{I}(\alpha_{lk} \neq 0) \right\}.$$

By Lemma 3, the eigenvalues of $\mathbf{K}_{\varphi,l}$ is of the order $O(\varphi M_n^{-1})$, we follow Taylor expansion and the third term denoted by T_3 of RHS of $V_{1(n)}^{(l)}(\mathbf{v})$ gives

$$\begin{aligned} T_3 &= \lambda_2 \left(\frac{M_n}{n} \right)^{1/2} \left\{ (\mathbf{v}^T \mathbf{K}_{\varphi,l} \mathbf{v})^{1/2} \mathbb{I}(\boldsymbol{\alpha}_l = \mathbf{0}) + \mathbf{v}^T (\boldsymbol{\alpha}_l^T \mathbf{K}_{\varphi,l} \boldsymbol{\alpha}_l)^{-1/2} \mathbf{K}_{\varphi,l} \boldsymbol{\alpha}_l \mathbb{I}(\boldsymbol{\alpha}_l \neq \mathbf{0}) \right\} + o\left(\frac{M_n}{n}\right) \lambda_2 \\ &= \lambda_2^2 n^{-1/2} \left\{ \|\mathbf{v}\|_2 \mathbb{I}(\boldsymbol{\alpha}_l = \mathbf{0}) + (\mathbf{v}^T \boldsymbol{\alpha}_l / \|\boldsymbol{\alpha}_l\|_2) \mathbb{I}(\boldsymbol{\alpha}_l \neq \mathbf{0}) \right\} + o\left(\frac{M_n}{n}\right) \lambda_2. \end{aligned}$$

So, we have $V_{1(n)}^{(l)}(\mathbf{v}) \xrightarrow{p} V_1^{(l)}(\mathbf{v})$ for a fixed \mathbf{v} . $V_1^{(l)}$ is a convex function. It follows the results of Geyer (1994) that $(n/M_n)^{1/2}(\hat{\mathbf{b}}_l - \boldsymbol{\alpha}_l) = \hat{\mathbf{v}}_n = \arg \min_{\mathbf{v}} V_{1(n)}^{(l)} \xrightarrow{p} \arg \min_{\mathbf{v}} V_1^{(l)}$. For $l = 1, \dots, J$, we multiply $\mathbf{B}_l(t)$ on both sides and obtain

$$\begin{aligned} (n/M_n)^{1/2}(\hat{\beta}_l(t) - \beta_l(t)) &= (n/M_n)^{1/2}(\hat{\beta}_l(t) - \beta_{\alpha l}(t)) + O(n^{1/2} M_n^{-\delta-1/2}) \\ &\xrightarrow{d} \mathbf{B}_l^T(t) \arg \min_{\mathbf{v}} V_1^{(l)}. \end{aligned}$$

4.3 Proof of Theorem 3

Proof of 1. Since finding $\hat{\mathcal{A}}_n = \mathcal{A}$ is the intersection of correctly estimating nonzero values for nonzero coefficient function and correctly identifying zero coefficient function, $P(\hat{\mathcal{A}}_n = \mathcal{A}) \leq P(\hat{\mathbf{b}}_l = \mathbf{0} \forall l \notin \mathcal{A})$. Let $\mathbf{v}_l^* = \arg \min_{\mathbf{v}_l} V_1^{(l)}(\mathbf{v}_l)$, Theorem 2 shows that $(n/M_n)^{1/2}(\hat{\mathbf{b}}_l - \boldsymbol{\alpha}_l) \xrightarrow{d} \mathbf{v}_l^*$. Therefore, we need to show that $c = P(\mathbf{v}_l^* = \mathbf{0} \forall l \notin \mathcal{A}) < 1$. There are two cases:

If $\gamma_1 = \gamma_2 = 0$, $\mathbf{v}_l^* = \mathbf{C}_l^{-1} \mathbf{W}_l \sim N(\mathbf{0}, \sigma^2 \mathbf{C}_l^{-1})$ and therefore $c = 0$.

If $\gamma_1 \neq 0$ or $\gamma_2 \neq 0$,

$$V_1^{(l)}(\mathbf{v}_l) = \begin{cases} \mathbf{v}_l^T \mathbf{C}_l \mathbf{v}_l - 2 \mathbf{W}_l^T \mathbf{v}_l + \gamma_1 \Gamma_1(\mathbf{v}_l) + \gamma_2 (\mathbf{v}_l^T \boldsymbol{\alpha}_l / \|\boldsymbol{\alpha}_l\|_2) & \text{if } l \in \mathcal{A} \\ \mathbf{v}_l^T \mathbf{C}_l \mathbf{v}_l - 2 \mathbf{W}_l^T \mathbf{v}_l + \gamma_1 \|\mathbf{v}_l\|_1 + \gamma_2 \|\mathbf{v}_l\|_2 & \text{if } l \notin \mathcal{A}, \end{cases}$$

where $\Gamma_1(\mathbf{v}_l) = \sum_{k=1}^{M_n+d} \left\{ |v_{lk}| \mathbb{I}(\alpha_{lk} = 0) + v_{lk} \text{sgn}(\alpha_{lk}) \mathbb{I}(\alpha_{lk} \neq 0) \right\}$. It can be seen that $V_1^{(l)}(\mathbf{v}_l)$ is not differentiable at $v_k = 0 \forall k$. By KKT condition of $V_1^{(l)}(\mathbf{v}_l)$,

$$\begin{cases} 2 \mathbf{C}_l \mathbf{v}_l^* - 2 \mathbf{W}_l + \gamma_1 \mathbf{p}_l + \gamma_2 \boldsymbol{\alpha}_l / \|\boldsymbol{\alpha}_l\|_2 = \mathbf{0} & \text{if } l \in \mathcal{A} \\ 2 \mathbf{C}_l \mathbf{v}_l^* - 2 \mathbf{W}_l + \gamma_1 \mathbf{q}_l + \gamma_2 \mathbf{z}_l = \mathbf{0} & \text{if } l \notin \mathcal{A}, \end{cases} \quad (\text{S8})$$

where $p_{lk} = \partial_{v_k} \{ |v_k| \mathbb{I}(\alpha_{lk} = 0) + v_k \text{sgn}(\alpha_{lk}) \mathbb{I}(\alpha_{lk} \neq 0) \}$,

$$q_{lk} = \begin{cases} \text{sgn}(v_k) & \text{if } v_k \neq 0 \\ \in \{q_{lk} : |q_{lk}| \leq 1\} & \text{if } v_k = 0, \end{cases} \quad \mathbf{z}_l = \begin{cases} \mathbf{v}_l / \|\mathbf{v}_l\|_2 & \text{if } \mathbf{v}_l \neq \mathbf{0} \\ \in \{\mathbf{z}_l : \|\mathbf{z}_l\|_2 \leq 1\} & \text{if } \mathbf{v}_l = \mathbf{0}. \end{cases}$$

The above discussion is regarding the individual coefficient function. To examine the variable selection consistency, we have to introduce new denotations by combining all coefficient functions. We let $\mathbf{C} = n^{-1} \mathbf{U}^T \mathbf{U}$, $\mathbf{U} = (\mathbf{U}_1, \dots, \mathbf{U}_J)^T$, $\mathbf{W} = (\mathbf{W}_1, \dots, \mathbf{W}_J)^T$, $\mathbf{p} = (\mathbf{p}_1, \dots, \mathbf{p}_J)^T$, $\mathbf{q} = (\mathbf{q}_1, \dots, \mathbf{q}_J)^T$, $\boldsymbol{\alpha} = (\boldsymbol{\alpha}_1, \dots, \boldsymbol{\alpha}_J)^T$, and $\mathbf{v}^* = (\mathbf{v}_1^*, \dots, \mathbf{v}_J^*)^T$. Without loss of generality, rewrite matrix \mathbf{C} in a block-wise form involving either $l \in \mathcal{A}$ or \mathcal{A}^c and rewrite vectors \mathbf{W} , \mathbf{p} , \mathbf{q} , $\boldsymbol{\alpha}$, and \mathbf{v}^* likewise, such that

$$\mathbf{C} = \begin{bmatrix} \mathbf{C}_{\mathcal{A}\mathcal{A}} & \mathbf{C}_{\mathcal{A}\mathcal{A}^c} \\ \mathbf{C}_{\mathcal{A}^c\mathcal{A}} & \mathbf{C}_{\mathcal{A}^c\mathcal{A}^c} \end{bmatrix}.$$

If $\mathbf{v}_l^* = \mathbf{0}$ for any $l \notin \mathcal{A}$, the optimality conditions (S8) become

$$\begin{cases} 2\mathbf{C}_{\mathcal{A}\mathcal{A}}\mathbf{v}_{\mathcal{A}}^* - 2\mathbf{W}_{\mathcal{A}} + \gamma_1\mathbf{p}_{\mathcal{A}} + \gamma_2\boldsymbol{\alpha}_{\mathcal{A}}/\|\boldsymbol{\alpha}_{\mathcal{A}}\|_2 = \mathbf{0} \\ \|\mathbf{C}_{\mathcal{A}^c\mathcal{A}}\mathbf{v}_{\mathcal{A}}^* - \mathbf{W}_{\mathcal{A}^c} + \gamma_1\mathbf{q}_{\mathcal{A}^c}\|_2 \leq \gamma_2. \end{cases} \quad (\text{S9})$$

Combining these optimality conditions (S9) above,

$$\left\| \mathbf{C}_{\mathcal{A}^c\mathcal{A}}\mathbf{C}_{\mathcal{A}\mathcal{A}}^{-1}(2\mathbf{W}_{\mathcal{A}} - \gamma_1\mathbf{p}_{\mathcal{A}} - \gamma_2\boldsymbol{\alpha}_{\mathcal{A}}/\|\boldsymbol{\alpha}_{\mathcal{A}}\|_2) - \mathbf{W}_{\mathcal{A}^c} + \gamma_1\mathbf{q}_{\mathcal{A}^c} \right\|_2 \leq \gamma_2.$$

Thus, we obtain,

$$c \leq P \left\{ \left\| \mathbf{C}_{\mathcal{A}^c\mathcal{A}}\mathbf{C}_{\mathcal{A}\mathcal{A}}^{-1}(2\mathbf{W}_{\mathcal{A}} - \gamma_1\mathbf{p}_{\mathcal{A}} - \gamma_2\boldsymbol{\alpha}_{\mathcal{A}}/\|\boldsymbol{\alpha}_{\mathcal{A}}\|_2) - \mathbf{W}_{\mathcal{A}^c} + \gamma_1\mathbf{q}_{\mathcal{A}^c} \right\|_2 \leq \gamma_2 \right\} < 1.$$

The first inequality is because we don't consider zero subregions for $l \in \mathcal{A}$. The second inequality is because the probability of irrepresentable conditions is strictly less than 1 (Zhao and Yu (2006)).

Proof of 2. Given the same reasoning of 1, $P(\hat{\beta}_l(t) = 0) \leq P(\hat{b}_{lk} = \mathbf{0} \ \forall k \notin \mathcal{B})$. We need to show that $c = P(\mathbf{v}_{lk}^* = \mathbf{0} \ \forall k \notin \mathcal{B}) < 1$. There are also two cases:

If $\gamma_1 = \gamma_2 = 0$, $\mathbf{v}_l^* = \mathbf{C}_l^{-1}\mathbf{W}_l \sim N(\mathbf{0}, \sigma^2\mathbf{C}_l^{-1})$ and therefore $c = 0$.

If $\gamma_1 = \gamma_2 = 0$, for $l \in \mathcal{A}$,

$$\begin{aligned} V_1^{(l)}(\mathbf{v}_l) &= \mathbf{v}_l^T \mathbf{C}_l \mathbf{v}_l - 2\mathbf{W}_l \mathbf{v}_l + \gamma_1 \Gamma_1(\mathbf{v}_l) + \gamma_2 \mathbf{v}_l^T \boldsymbol{\alpha}_{\mathcal{A}} / \|\boldsymbol{\alpha}_{\mathcal{A}}\|_2 \\ &= \begin{cases} \mathbf{v}_l^T \mathbf{C}_l \mathbf{v}_l - 2\mathbf{W}_l \mathbf{v}_l + \gamma_1 v_{lk} \text{sgn}(\alpha_{lk}) + \gamma_2 \mathbf{v}_l^T \boldsymbol{\alpha}_{\mathcal{A}} / \|\boldsymbol{\alpha}_{\mathcal{A}}\|_2 & \text{if } k \in \mathcal{B} \\ \mathbf{v}_l^T \mathbf{C}_l \mathbf{v}_l - 2\mathbf{W}_l \mathbf{v}_l + \gamma_1 |v_{lk}| + \gamma_2 \mathbf{v}_l^T \boldsymbol{\alpha}_{\mathcal{A}} / \|\boldsymbol{\alpha}_{\mathcal{A}}\|_2 & \text{if } k \notin \mathcal{B}. \end{cases} \end{aligned}$$

We can follow the KKT conditions with respect to individual v_{lk} , and then depend on the similar reasoning of the proof of 1 to obtain the results.

4.4 Proof of Theorem 4

The proof of Theorem 4 requires Lemma 4, which shows the rate of convergence of initial estimator which is derived from penalized B-splines estimator in Cardot et al. (2003). Let λ be the tuning parameter for the functional generalization of ridge regularization.

Lemma 4. *Under (A.1)-(A.2), if $\lambda = O(M_n^{-1/2} n^{-1/2})$, $\|\hat{\beta}_l - \beta_l\|_{\infty} = O_p(M_n^{1/2} n^{-1/2})$.*

Proof. The proof depends on the identical procedure as Theorem 1.

Now we are ready to show the proof of Theorem 4. According to (S3), we define $Q(\mathbf{v})$ by adding adaptive weights as following

$$\begin{aligned} Q(\mathbf{v}) &= \|\mathbf{r}_{(-l)} - \mathbf{U}_l(\boldsymbol{\alpha}_l + (M_n/n)^{1/2} \mathbf{v})\|_2^2 + \Delta_n \lambda_1 \hat{w}_l^{(1)} \|\boldsymbol{\alpha}_l + (M_n/n)^{1/2} \mathbf{v}\|_1 + \\ &\quad \lambda_2 \hat{w}_l^{(2)} ((\boldsymbol{\alpha}_l + (M_n/n)^{1/2} \mathbf{v})^T \mathbf{K}_{\varphi, l} (\boldsymbol{\alpha}_l + (M_n/n)^{1/2} \mathbf{v}))^{1/2}. \end{aligned}$$

Suppose the minimizer of $Q(\mathbf{v})$ is noted as $\hat{\mathbf{v}}_n$, then $\hat{\mathbf{v}}_n = (n/M_n)^{1/2}(\hat{\mathbf{b}}_l - \boldsymbol{\alpha}_l)$. We need to show the limiting distribution of $\hat{\mathbf{v}}_n$. Note that $V_{2(n)}^{(l)}(\mathbf{v}) = Q(\mathbf{v}) - Q(\mathbf{0})$, where

$$V_{2(n)}^{(l)}(\mathbf{v}) = \begin{cases} \mathbf{v}^T \mathbf{C}_l \mathbf{v} - 2\mathbf{W}_l^T \mathbf{v} + \Delta_n \lambda_1 (\frac{M_n}{n})^{1/2} \hat{w}_l^{(1)} \sum_{k=1}^{M_n+d} \left\{ |v_k| \mathbb{I}(\alpha_k = 0) + \right. \\ \left. v_k \text{sgn}(\alpha_k) \mathbb{I}(\alpha_k \neq 0) \right\} + \lambda_2 (\frac{M_n}{n})^{1/2} \hat{w}_l^{(2)} \mathbf{v}^T (\boldsymbol{\alpha}_l^T \mathbf{K}_{\varphi, l} \boldsymbol{\alpha}_l)^{-1/2} \mathbf{K}_{\varphi, l} \boldsymbol{\alpha}_l & \text{if } l \in \mathcal{A} \\ \mathbf{v}^T \mathbf{C}_l \mathbf{v} - 2\mathbf{W}_l^T \mathbf{v} + \Delta_n \lambda_1 (\frac{M_n}{n})^{1/2} \hat{w}_l^{(1)} \|\mathbf{v}\|_1 + \lambda_2 (\frac{M_n}{n})^{1/2} \hat{w}_l^{(2)} (\mathbf{v}^T \mathbf{K}_{\varphi, l} \mathbf{v})^{1/2} & \text{if } l \notin \mathcal{A}, \end{cases}$$

where $(M_n/n) \mathbf{U}_l^T \mathbf{U}_l \rightarrow \mathbf{C}_l$ and $\mathbf{W}_l = N(\mathbf{0}, \sigma^2 \mathbf{C}_l)$ as before.

If $l \notin \mathcal{A}$, $\hat{w}_l^{(1)} = \|\hat{\beta}\|_1^{-a} = O_p(M_n^{-a/2} n^{a/2})$ and $\hat{w}_l^{(2)} = \|\hat{\beta}\|_2^{-a} = O_p(M_n^{-a/2} n^{a/2})$, then

$$\Delta_n \lambda_1 \left(\frac{M_n}{n}\right)^{1/2} \hat{w}_l^{(1)} \|\mathbf{v}\|_1 \propto \frac{\lambda_1}{(nM_n)^{1/2}} \frac{n^{a/2}}{M_n^{a/2}} \hat{w}_l^{(1)} \frac{M_n^{a/2}}{n^{a/2}} \|\mathbf{v}\|_1 = \frac{\lambda_1 n^{(a-1)/2}}{M_n^{(a+1)/2}} \hat{w}_l^{(1)} \frac{M_n^{a/2}}{n^{a/2}} \|\mathbf{v}\|_1 \xrightarrow{p} \infty,$$

since $\lambda_1 n^{(a-1)/2} / M_n^{(a+1)/2} \rightarrow \infty$ and $(M_n^{a/2} / n^{a/2}) \hat{w}_l^{(1)} = O_p(1)$; by Lemma 3, $(\mathbf{v}^T \mathbf{K}_{\varphi,l} \mathbf{v})^{1/2} = O(\lambda_2 M_n^{-1/2})$, then

$$\lambda_2 \left(\frac{M_n}{n}\right)^{1/2} \hat{w}_l^{(2)} (\mathbf{v}^T \mathbf{K}_{\varphi,l} \mathbf{v})^{1/2} = \frac{\lambda_2^2 n^{(a-1)/2}}{M_n^{a/2}} \hat{w}_l^{(2)} \frac{M_n^{a/2}}{n^{a/2}} \xrightarrow{p} \infty,$$

since $\lambda_2^2 n^{(a-1)/2} / M_n^{a/2} \rightarrow \infty$ and $(M_n^{a/2} / n^{a/2}) \hat{w}_l^{(2)} = O_p(1)$. Hence, for $l \notin \mathcal{A}$

$$V_{2(n)}^{(l)}(\mathbf{v}) = \infty. \quad (\text{S10})$$

If $l \in \mathcal{A}$, we have

$$V_{2(n)}^{(l)}(\mathbf{v}) = \begin{cases} \mathbf{v}^T \mathbf{C}_l \mathbf{v} - 2 \mathbf{W}_l^T \mathbf{v} + \Delta_n \lambda_1 \left(\frac{M_n}{n}\right)^{1/2} \hat{w}_l^{(1)} v_k \text{sgn}(\alpha_k) + \\ \lambda_2 \left(\frac{M_n}{n}\right)^{1/2} \hat{w}_l^{(2)} \mathbf{v}^T (\boldsymbol{\alpha}_l^T \mathbf{K}_{\varphi,l} \boldsymbol{\alpha}_l)^{-1/2} \mathbf{K}_{\varphi,l} \boldsymbol{\alpha}_l & \text{if } k \in \mathcal{B} \\ \mathbf{v}^T \mathbf{C}_l \mathbf{v} - 2 \mathbf{W}_l^T \mathbf{v} + \Delta_n \lambda_1 \left(\frac{M_n}{n}\right)^{1/2} \hat{w}_l^{(1)} |v_k| + \\ \lambda_2 \left(\frac{M_n}{n}\right)^{1/2} \hat{w}_l^{(2)} \mathbf{v}^T (\boldsymbol{\alpha}_l^T \mathbf{K}_{\varphi,l} \boldsymbol{\alpha}_l)^{-1/2} \mathbf{K}_{\varphi,l} \boldsymbol{\alpha}_l & \text{if } k \notin \mathcal{B}. \end{cases}$$

Following the same arguments before, when $k \notin \mathcal{B}$, we know that $\Delta_n \lambda_1 \left(\frac{M_n}{n}\right)^{1/2} \hat{w}_l^{(1)} |v_k| \xrightarrow{p} \infty$ and $\lambda_2 \left(\frac{M_n}{n}\right)^{1/2} \hat{w}_l^{(2)} \mathbf{v}^T (\boldsymbol{\alpha}_l^T \mathbf{K}_{\varphi,l} \boldsymbol{\alpha}_l)^{-1/2} \mathbf{K}_{\varphi,l} \boldsymbol{\alpha}_l \xrightarrow{p} \infty$ if $\lambda_1 n^{(a-1)/2} / M_n^{(a+1)/2} \rightarrow \infty$ and $\lambda_2^2 n^{(a-1)/2} / M_n^{a/2} \rightarrow \infty$, as $(\boldsymbol{\alpha}_l^T \mathbf{K}_{\varphi,l} \boldsymbol{\alpha}_l)^{-1/2} \mathbf{K}_{\varphi,l} \boldsymbol{\alpha}_l = O(\lambda_2 M_n^{-1/2})$ by Lemma 3 again. Let \mathbf{v} be re-expressed in a blockwise form mentioned before, $\mathbf{v} = (\mathbf{v}_{\mathcal{B}}, \mathbf{v}_{\mathcal{B}^c})^T$. Hence, for $l \notin \mathcal{A}$ and $k \notin \mathcal{B}$,

$$V_{2(n)}^{(l)}(\mathbf{v}_{\mathcal{B}^c}) = \infty. \quad (\text{S11})$$

When considering $l \in \mathcal{A}$ and $k \in \mathcal{B}$, that is, $t \in I_0(\beta_l)$, $\hat{\beta}_l(t) \xrightarrow{p} \beta_l(t) \neq 0$. Therefore, the last two terms converge to zero in probability under the conditions $\lambda_1 (nM_n)^{-1/2} \rightarrow 0$ and $\lambda_2^2 n^{-1/2} \rightarrow 0$. For $l \notin \mathcal{A}$ and $k \in \mathcal{B}$,

$$V_{2(n)}^{(l)}(\mathbf{v}_{\mathcal{B}}) = \mathbf{v}_{\mathcal{B}}^T (\mathbf{C}_l)_{\mathcal{B}\mathcal{B}} \mathbf{v}_{\mathcal{B}} - 2 (\mathbf{W}_l)_{\mathcal{B}}^T \mathbf{v}_{\mathcal{B}}. \quad (\text{S12})$$

Thus, we see that $V_{2(n)}^{(l)}(\mathbf{v}) \xrightarrow{p} V_2^{(l)}(\mathbf{v})$ for a fixed \mathbf{v} and $V_{2(n)}^{(l)}$ is a convex function. Given (S10), (S11), and (S12), it follows the results of Geyer (1994) that $\hat{\mathbf{v}}_n^{(l)} = \arg \min_{\mathbf{v}} V_{2(n)}^{(l)} \xrightarrow{p} \arg \min_{\mathbf{v}} V_2^{(l)}$, where

$$V_2^{(l)}(\mathbf{v}) = \begin{cases} \mathbf{v}_{\mathcal{B}}^{(l)T} \mathbf{C}_{l\mathcal{B}\mathcal{B}} \mathbf{v}_{\mathcal{B}}^{(l)} - 2\mathbf{W}_{l\mathcal{B}}^T \mathbf{v}_{\mathcal{B}}^{(l)} & \text{if } l \in \mathcal{A} \text{ \& } k \in \mathcal{B} \\ \infty & \text{if } l \in \mathcal{A} \text{ \& } k \notin \mathcal{B} \\ \infty & \text{if } l \notin \mathcal{A}, \end{cases}$$

and $\mathbf{C}_{l\mathcal{B}\mathcal{B}}$, $\mathbf{W}_{l\mathcal{B}}$ are similarly defined. Therefore, we have $\hat{\mathbf{v}}_{nk}^{(l)} \xrightarrow{d} \mathbf{C}_{l\mathcal{B}\mathcal{B}}^{-1} \mathbf{W}_{l\mathcal{B}}$ if $l \in \mathcal{A}$ and $k \in \mathcal{B}$; $\hat{\mathbf{v}}_{nk}^{(l)} \xrightarrow{d} \mathbf{0}$ if $l \in \mathcal{A}$ and $k \notin \mathcal{B}$; $\hat{\mathbf{v}}_{nk}^{(l)} \xrightarrow{d} \mathbf{0}$ if $l \notin \mathcal{A}$. Since $\mathbf{W}_{l\mathcal{B}} \sim N(\mathbf{0}, \sigma^2 \mathbf{C}_{l\mathcal{B}\mathcal{B}})$, it can be seen that for $t \in I_1(\beta_l)$,

$$\begin{aligned} (n/M_n)^{1/2}(\hat{\beta}_l(t) - \beta_l(t)) &= (n/M_n)^{1/2}(\hat{\beta}_l(t) - \beta_{al}(t)) + (n/M_n)^{1/2}(\beta_{al}(t) - \beta_l(t)) \\ &= (n/M_n)^{1/2} \mathbf{B}_l^T (\hat{\mathbf{b}}_{l\mathcal{B}} - \boldsymbol{\alpha}_{l\mathcal{B}}) + O(n^{1/2} M_n^{-\delta-1/2}) \\ &\xrightarrow{d} \mathbf{B}_l^T \mathbf{C}_{l\mathcal{B}\mathcal{B}}^{-1} \mathbf{W}_{l\mathcal{B}} \\ &\xrightarrow{d} N(0, \Sigma_{lt}), \end{aligned}$$

where $\Sigma_{lt} = \sigma^2 \mathbf{B}_l^T(t) \mathbf{C}_{l\mathcal{B}\mathcal{B}}^{-1} \mathbf{B}_l(t)$.

We now want to prove the consistency of global and local selection. We start with the global variable selection. When $l \in \mathcal{A}$, $\beta_l(t) \neq 0$ at least at one time point t . The asymptotic normality indicates that $P(l \in \hat{\mathcal{A}}) \rightarrow 1$. Then it suffices to show that $\forall l' \notin \mathcal{A}$, $P(l' \in \hat{\mathcal{A}}) \rightarrow 0$. We rewrite the objective function for $\mathbf{b}_{l'}$, resulting in $L_n(\mathbf{b}_{l'}) = \|\mathbf{r}_{(-l')} - \mathbf{U}_{l'} \mathbf{b}_{l'}\|_2^2 + \Delta_n \lambda_1 \hat{w}_{l'}^{(1)} \|\mathbf{b}_{l'}\|_1 + \lambda_2 \hat{w}_{l'}^{(2)} (\mathbf{b}_{l'}^T \mathbf{K}_{l'} \mathbf{b}_{l'})^{1/2}$.

If $l' \in \hat{\mathcal{A}}$, by Lemma 3 and KKT conditions, we have

$$2\mathbf{U}_{l'}^T (\mathbf{r}_{(-l')} - \mathbf{U}_{l'} \mathbf{b}_{l'}) = \Delta_n \lambda_1 \hat{w}_{l'}^{(1)} \mathbf{q}_{l'} + \lambda_2 M_n^{-1/2} \hat{w}_{l'}^{(2)} \mathbf{b}_{l'} / \|\mathbf{b}_{l'}\|_2 \quad (\text{S13})$$

where

$$\mathbf{q}_{l'k} = \begin{cases} \text{sgn}(b_{l'k}) & \text{if } b_{l'k} \neq 0 \\ \in \{q_{l'k} : |q_{l'k}| \leq 1\} & \text{if } b_{l'k} = 0. \end{cases}$$

Multiplying $(M_n/n)^{1/2}$ on both sides, Equation (S13) gives $(M_n/n)^{1/2} \Delta_n \lambda_1 \hat{w}_{l'}^{(1)} \xrightarrow{p} \infty$ and

$(M_n/n)^{1/2}\lambda_2^2M_n^{-1/2}\hat{w}_l^{(2)} \xrightarrow{p} \infty$ under the conditions, while

$$\begin{aligned} 2(M_n/n)^{1/2}\mathbf{U}_{l'}^T(\mathbf{r}_{(-l')} - \mathbf{U}_{l'}\mathbf{b}_{l'}) &= 2(M_n/n)^{1/2}(\mathbf{U}_{l'}^T(\mathbf{r}_{(-l')} - \mathbf{U}_{l'}\boldsymbol{\alpha}_{l'} + \mathbf{U}_{l'}\boldsymbol{\alpha}_{l'} - \mathbf{U}_{l'}\mathbf{b}_{l'})) \\ &= 2\mathbf{W}_{l'} + 2(M_n/n)\mathbf{U}_{l'}^T\mathbf{U}_{l'}(n/M_n)^{1/2}(\boldsymbol{\alpha}_{l'} - \mathbf{b}_{l'}). \end{aligned}$$

It can be told that $\mathbf{W}_{l'}$ follows $N(0, \sigma^2\mathbf{C}_{l'})$ and the second term asymptotically converges to normal distribution. By Slutsky's theorem, $2(M_n/n)^{1/2}\mathbf{U}_{l'}^T(\mathbf{r}_{(-l')} - \mathbf{U}_{l'}\mathbf{b}_{l'}) \xrightarrow{d}$ some normal distribution. Therefore,

$$P(l' \in \hat{\mathcal{A}}) \leq P\{2\mathbf{U}_{l'}^T(\mathbf{r}_{(-l')} - \mathbf{U}_{l'}\mathbf{b}_{l'}) = \Delta_n\lambda_1\hat{w}_{l'}^{(1)}\mathbf{y}_{l'} + \lambda_2^2M_n^{-1/2}\hat{w}_{l'}^{(2)}\mathbf{b}_{l'}/\|\mathbf{b}_{l'}\|_2\} \rightarrow 0$$

Now we want to prove the consistency of local selection only considering $l \in \mathcal{A}$ and $t \in I_0(\beta_l)$, which means $\alpha_k \neq 0$ for $k \in \mathcal{B}$. The asymptotic normality indicates that $P(k \in \hat{\mathcal{B}}|l \in \mathcal{A}) \rightarrow 1$. Then it suffices to show that $\forall k' \notin \mathcal{B}$, $P(k' \in \hat{\mathcal{B}}|l \in \mathcal{A}) \rightarrow 0$.

If $k' \in \hat{\mathcal{B}}$, by Lemma 3 and KKT conditions, we have

$$2\mathbf{U}_l^T(\mathbf{r}_{(-l)} - \mathbf{U}_l\mathbf{b}_l)I_{k'} = \Delta_n\lambda_1\hat{w}_l^{(1)}\text{sgn}(b_{lk'}) + \lambda_2^2M_n^{-1/2}\hat{w}_l^{(2)}b_{lk'}/\|\mathbf{b}_l\|_2,$$

where $I_{k'}$ denotes $(M_n + d)$ -dimensional unit vector with 1 at the k' th entry. Following the similar reasoning as above, the RHS tends to be infinite while the LHS is asymptotically normal. Hence,

$$P(k' \in \hat{\mathcal{B}}|l \in \hat{\mathcal{A}}) \leq P(2(\mathbf{U}_l^T(\mathbf{r}_{(-l)} - \mathbf{U}_l\mathbf{b}_l))I_{k'} = \Delta_n\lambda_1\hat{w}_l^{(1)}\text{sgn}(b_{lk'}) + \lambda_2^2\hat{w}_l^{(2)}b_{lk'}/\|\mathbf{b}_l\|_2) \rightarrow 0$$

References

- Cardot, H., Ferraty, F., and Sarda, P. (2003). Spline estimators for the functional linear model. *Statistica Sinica*, 13:571–791.
- De Boor, C. (2001). *A Practical Guide to Splines*. Springer.
- Geyer, C. (1994). On the asymptotics of constrained m-estimation. *The Annals of Statistics*, 22:1993–2010.

- Huang, J. Z., Wu, C. O., and Zhou, L. (2004). Polynomial spline estimation and inference for varying coefficient models with longitudinal data. *Statistica Sinica*, 14:763–788.
- Lin, Z., Cao, J., Wang, L., and et al. (2017). Locally sparse estimator for functional linear regression models. *Journal of Computational and Graphical Statistics*, 26(2):306–318.
- Wang, X. and Yuan, X. (2012). The linearized alternating direction method for dantzig selector. *SIAM Journal on Scientific Computing*, 34:A2792–A2811.
- Zhao, P. and Yu, B. (2006). On model selection consistency of lasso. *Journal of Machine Learning Research*, 7:2541–2567.
- Zhou, J., Wang, N., and Wang, N. (2013). Functional linear model with zero-value coefficient function at sub-regions. *Statistica Sinica*, 23(1):25–50.